Characteristics and origin of oil and gas in the Nanpu sag, Bohai Bay Basin, China: Insights from oil-source correlation and source rock effects

Gang Gao, Jianyu Zhao, Shangru Yang, Wenzhe Gang, Yuexia Dong, and Zhongxin Zhao

ABSTRACT

The Nanpu sag is a typical petroliferous area in the Bohai Bay Basin. Crude oil density and viscosity, natural gas components and biomarker chemistry of crude oil, and shale sample extracts were analyzed to determine the characteristics and the origin of oil and gas and the effects of source rock on oil and gas distribution. The discovered heavy oil present in the shallow layers of the Liuzan, Gaoshangpu, and Laoyemiao regions are a product of biodegradation and oxidation. The crude oil samples from the offshore locations are low density and viscosity, indicating good preservation conditions. Biomarker compositions indicate that the crude oils can be divided into four types: A, B, C, and D. Both type A and D oils were sourced from the third member of the Shahejie Formation. Type A oil is primarily distributed in the Liuzan and Gaoshangpu regions, whereas type D oil is chiefly distributed in the nos. 1, 2, 5, and Beipu structural belts (SBs). Type B oil, derived from the third member of the Dongying Formation, is primarily distributed in the Laoyemiao, Gaonan, and Liunan SBs. The type C oil is primarily derived from the first member of the Shahejie Formation and is distributed in the Beipu and nos. 1–4 SBs. The hydrocarbons are primarily distributed in the regions where the thick source rocks interact with faults. The discovered natural gas in the Nanpu sag is primarily observed as dissolved gas in oil and free gas.

Manuscript received November 19, 2017; provisional acceptance January 11, 2018; revised manuscript received June 25, 2018; revised manuscript provisional acceptance July 30, 2018; 2nd revised manuscript received February 21, 2019; 2nd revised manuscript provisional acceptance March 12, 2019; 3rd revised manuscript received June 25, 2019; 3rd revised manuscript provisional acceptance July 25, 2019; 4th revised manuscript received April 26, 2020; 4th revised manuscript provisional acceptance May 8, 2020; 5th revised manuscript received May 14, 2020; final acceptance November 19, 2020.

DOI:10.1306/01152117395

AUTHORS

GANG GAO ~ *State Key Laboratory of Petroleum Resources and Prospecting, China University of Petroleum (Beijing), Beijing, China; College of Geosciences, China University of Petroleum (Beijing), Beijing, China; present address: Department of Petroleum Exploration and Development Geology, China University of Petroleum (Beijing), Beijing, China; gaogang2819@sina.com*

Gao Gang received his Ph.D. from the China University of Mining and Technology, Beijing, in 2005. He is now an associate professor at the China University of Petroleum (Beijing). His current research interests are oil and gas accumulation mechanism and regularity of distribution. He is the corresponding author.

JIANYU ZHAO ~ *State Key Laboratory of Petroleum Resources and Prospecting, China University of Petroleum (Beijing), Beijing, China; College of Geosciences, China University of Petroleum (Beijing), Beijing, China; 11670089@qq.com*

Jianyu Zhao received his bachelor's degree from Southwest Petroleum University, Chengdu, China, in 2018. He is now studying for a master's degree at China University of Petroleum (Beijing). His current research interests include petroleum geochemistry and hydrocarbon migration.

SHANGRU YANG ~ *State Key Laboratory of Petroleum Resources and Prospecting, China University of Petroleum (Beijing), Beijing, China; College of Geosciences, China University of Petroleum (Beijing), Beijing, China; yangshangru1992@163.com*

Shangru Yang received his master's degree from China University of Petroleum (Beijing), in 2018. He is now studying for a doctorate at China University of Petroleum (Beijing). His current research interests include petroleum geochemistry and hydrocarbon migration.

WENZHE GANG ~ *State Key Laboratory of Petroleum Resources and Prospecting, China University of Petroleum (Beijing), Beijing, China; College of Geosciences, China University of Petroleum (Beijing), Beijing, China; present address: Department of*

Petroleum Exploration and Development Geology, China University of Petroleum (Beijing), Beijing, China; gwz@cup.edu.com.

Wenzhe Gang received his Ph.D. from the China University of Petroleum (Beijing), in 1996. He is now a professor at the China University of Petroleum (Beijing). His current research interests are petroleum geochemistry and hydrocarbon migration.

YUEXIA DONG ~ *Exploration and Development Research Institute, Jidong Oilfield Company, China National Petroleum Corporation (CNPC), Tangshan, China; dongyx@petrochina.com.*

Yuexia Dong received her Ph.D. from the China University of Geosciences, Wuhan, in 2002. She is now a senior engineer at professor grade and chief geologist of Jidong Oilfield Company. Her current research interests are petroleum exploration geology and production.

ZHONGXIN ZHAO ~ *Exploration and Development Research Institute, Jidong Oilfield Company, CNPC, Tangshan, China; jd_zzx@petrochina.com.cn.*

Zhongxin Zhao received his Ph.D. from the China University of Geosciences, Wuhan, in 2006. He is now a deputy chief geologist in the Exploration and Development Research Institute of the Jidong Oilfield Company. His current research interests are petroleum exploration geology and production.

ACKNOWLEDGMENTS

This study was jointly supported by grants from the Key National Project (Grant No. 2016ZX05006-006) and the National Natural Science Foundation of China (No. 41372142). We acknowledge the Jidong Oilfield Company, CNPC, for allowing the publication of this manuscript and providing data and a stratigraphic framework.

INTRODUCTION

The Nanpu sag is rich in oil and gas resources. Petroleum has been found in the basement and in all sedimentary units from the Paleogene to the Neogene with different oil and gas abundances (Dong et al., 2003, 2010; Mei et al., 2008). In onshore structural belts (SBs), there is a very high level of exploration (including the Laoyemiao, Gaoshangpu, Liuzan, and Beipu SBs). Recently, considerable oil and gas resources have been discovered in offshore SBs (Nanpu nos. 1–5 SBs), indicating significant petroleum exploration potential (Dong et al., 2010). The existing source rock studies have examined the origin of oil and gas focusing on a specific SB rather than the whole Nanpu sag (Mei et al., 2008; Zhao et al., 2008). Issues such as depth distribution, origin and spatial distribution of the different oil and gas families, distribution of source rock, and controls on the accumulation and distribution of the oil and gas need to be examined (Li et al., 2008; Mei et al., 2008; Zhao et al., 2008; Jiang et al., 2016a, b, c).

New crude oil and shale samples were collected and analyzed from the whole Nanpu sag. In addition, the oil and gas accumulation distribution, physical properties, type and source of the crude oil, composition of the natural gas, thermal maturity, and depositional environment of source rock are comprehensively analyzed to determine the effect of source rock on the oil and gas distribution in the entire Nanpu sag in this paper. Based on the analysis of crude oil and source rocks in the Nanpu sag of Bohai Bay Basin, this paper provides a research method for the exploration of oil and gas fields in other rift basins. The geochemical characteristics of crude oil combined with the macroscopic distribution of source rocks can predict the favorable spatial distribution of crude oil under the influence of faults. At the same time, this is a reversible analytical approach, based on the characteristics of the discovered oil field, to infer the range of possible control effective source rocks.

GEOLOGICAL SETTING

Tectonics

The Nanpu sag is located in the northeastern Huanghua depression of the Bohai Bay Basin in North China, covering an area of approximately 1900 km^2 (~730 mi^2). The onshore and the offshore areas are 540 and 1360 km^2 (~210 and 530 mi^2), respectively (Liu et al., 2009; Wan et al., 2012). The Nanpu sag is bounded to the northwest by the Laowangzhuang and Xi'nanzhuang uplifts, to the northeast by the Baigezhuang and Matouying uplifts, and to the south by the Shaleitian uplift (Shi et al., 2011; Zhou et al., 2011) (Figure 1). The subsags and

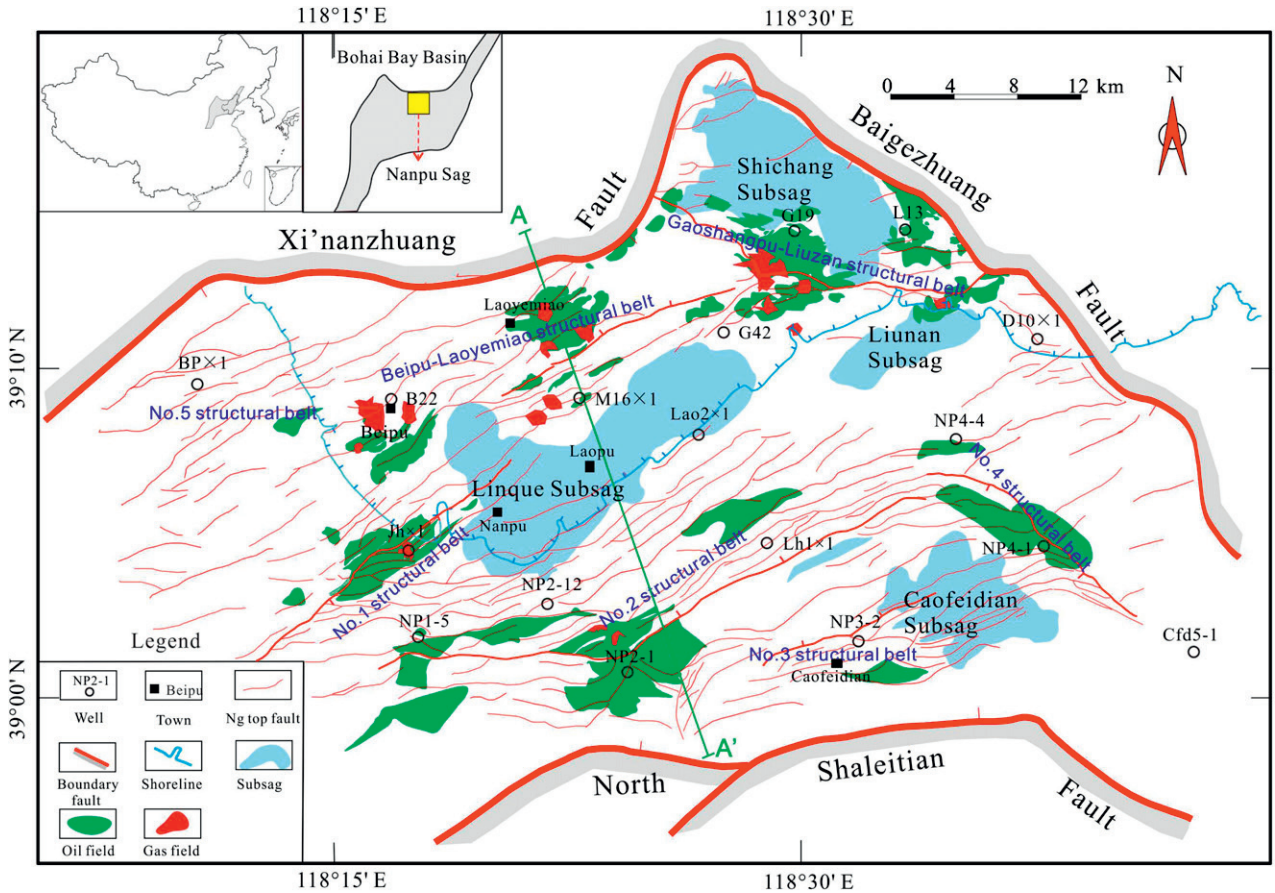

Figure 1. Location map, structural units, and distribution of the oil and gas fields in the Nanpu sag. AA′ is the north-northwest structural section in the Nanpu sag. Ng = Neogene Guantao Formation.

structure belts are controlled by third-order faults, such as the Gaoliu, Miaonan, Laopu, and Hatuo faults (Li et al., 2010). The sag contains the following structural elements: (1) four subsags (Shichang, Linque, Liunan, and Caofeidian subsags), (2) onshore SBs, and (3) offshore SBs (Figure 1). Figure 2 shows a typical section across the Nanpu sag with a north-northwest direction.

The Nanpu sag experienced a synrift stage during the Paleogene and a postrift stage during the Neogene (Xu et al., 2008; Dong et al., 2010; Chen et al., 2016) (Figure 3). The synrift stage can be subdivided into episodes I, II, and III (Guo et al., 2013). There existed two directions of extension (northwest-southeast, followed by north-south direction) that were closely related to the direction change of the Pacific plate movement (ca. 40 Ma) (Tong et al., 2013). During episode I, the Nanpu sag experienced northwest-southeast direction extension, following preexisting Mesozoic weaknesses. This was followed by north-south extension following preexisting faults. Therefore, there are extensional normal faults trending to the northeast and northeast-east, with numerous tensional-shear faults that are locally observed with Y-shaped, X-shaped, and step fault styles in the section (Tong et al., 2013) (Figure 2).

Stratigraphy and Paleogeography

In the Nanpu sag, the Cenozoic sedimentary strata are composed of the Paleogene Shahejie and Dongying Formations, Neogene Guantao (Ng) and Minghuazhen (Nm) Formations, and the Quaternary Pingyuan Formation, with a maximum thickness of 7500 m (24,600 ft) (Dong et al., 2003) (Figure 3).

The Shahejie Formation is lacustrine to deltaic and has been subdivided into three members: Es_1, Es_2, and Es_3 from top to bottom based on lithologic characteristics. The Es_1 was deposited in a lacustrine-delta sedimentary environment, with relatively weak

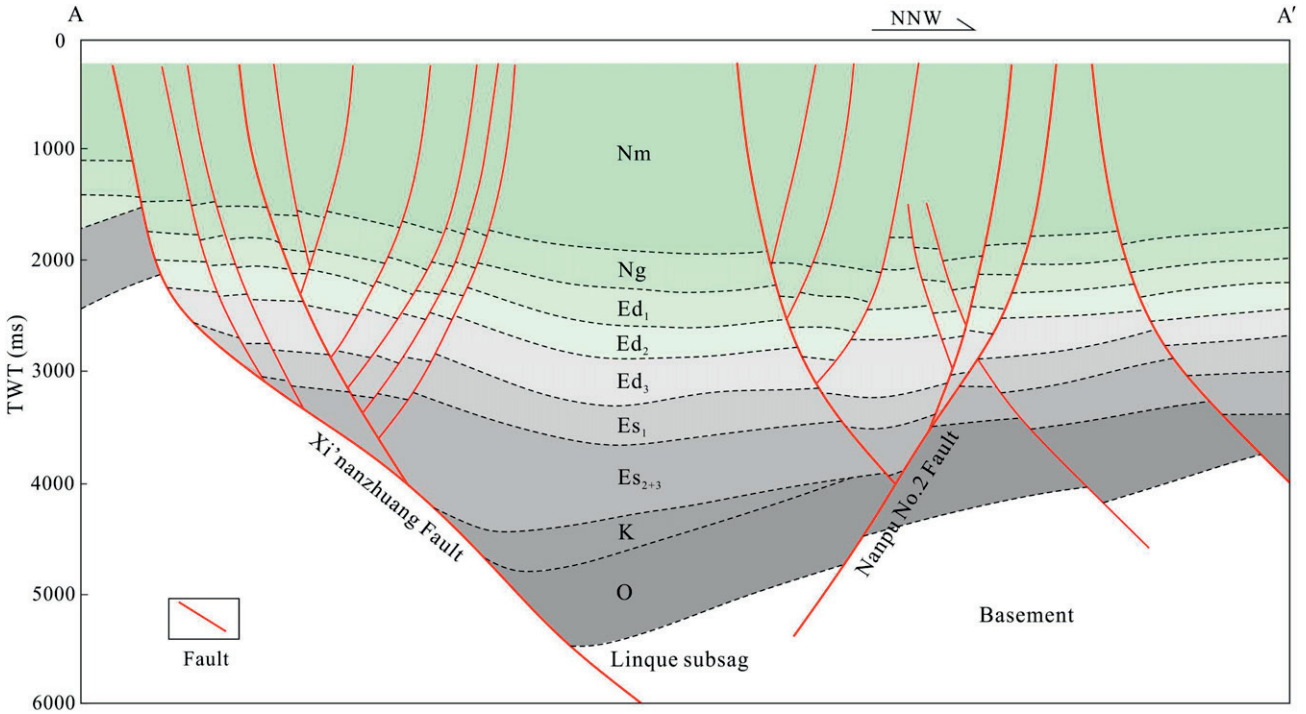

Figure 2. Structural section (AA′) in the Nanpu sag. Ed_1 = first member of the Dongying Formation; Ed_{2+3} = second member + third member of the Dongying Formation; Ed_3 = third member of the Dongying Formation; Es_1 = first member of the Shahejie Formation; Es_{2+3} = second member + third member of the Shahejie Formation; K = Cretaceous; Ng = Neogene Guantao Formation; Nm = Neogene Minghuazhen Formation; O = Ordovician; TWT = vertical two-way traveltime.

tectonic activity. It is composed of a gray coarse-grained sandstone, fine-grained sandstone, siltstone, and grayish and dark gray shale (Figure 3). The Es_2 contains thinner conglomerate and mudstone, which were eroded in most of the Nanpu sag because of basement uplifting. The Es_3 comprises thick dark gray and gray-black shale with thin layers of sandstone, especially within the Gaoshangpu and Liuzan SBs.

The Dongying Formation was mainly deposited in a fan delta and deltaic sedimentary environment and has been subdivided into three members: Ed_1, Ed_2, and Ed_3 (Jiang et al., 2009; Chen et al., 2016) (Figure 3). The Ed_1 comprises a gray shale, pebbled sandstone, and sandstone; the Ed_2 consists of a gray shale, pebbled sandstone, and fine-grained sandstone; and the Ed_3 is composed of a gray conglomerate, pebbled sandstone, and gray shale.

The Ng consists of braided river deposits with a conglomerate, sandy conglomerate, basic volcanic rock, and thin gray-green and gray shale.

The Nm is a set of meandering river deposits with shale and massive sandstone (Zhang et al., 2010) (Figure 3). Quaternary Pingyuan Formation consists of terrigenous detrital deposits, with the depocenter being located in the Laopu-Hatuo area.

MATERIALS AND METHODS

Crude-oil density and viscosity data were collected from the Jidong Oilfield Company, China National Petroleum Corporation. The 58 natural gas samples were obtained by a drainage method under saturated salt water. The geochemical data are listed in Table 1. The molecular composition was analyzed for both oil and gas samples by the State Key Laboratory of Petroleum Resource and Prospecting, China University of Petroleum, Beijing. An Agilent 6890N gas chromatograph (GC) equipped with flame ionization and thermal conductivity detectors was used to determine the molecular composition of the natural gas samples. The hydrocarbon gas components were separated by using a capillary column (PLOT Al_2O_3, 50 m × 0.53 mm). Helium (99.999%) was used as the carrier gas with a constant flow of 0.3 ml/min. The injection temperature was 200°C. The column oven was maintained at 30°C for 10 min, then increased from

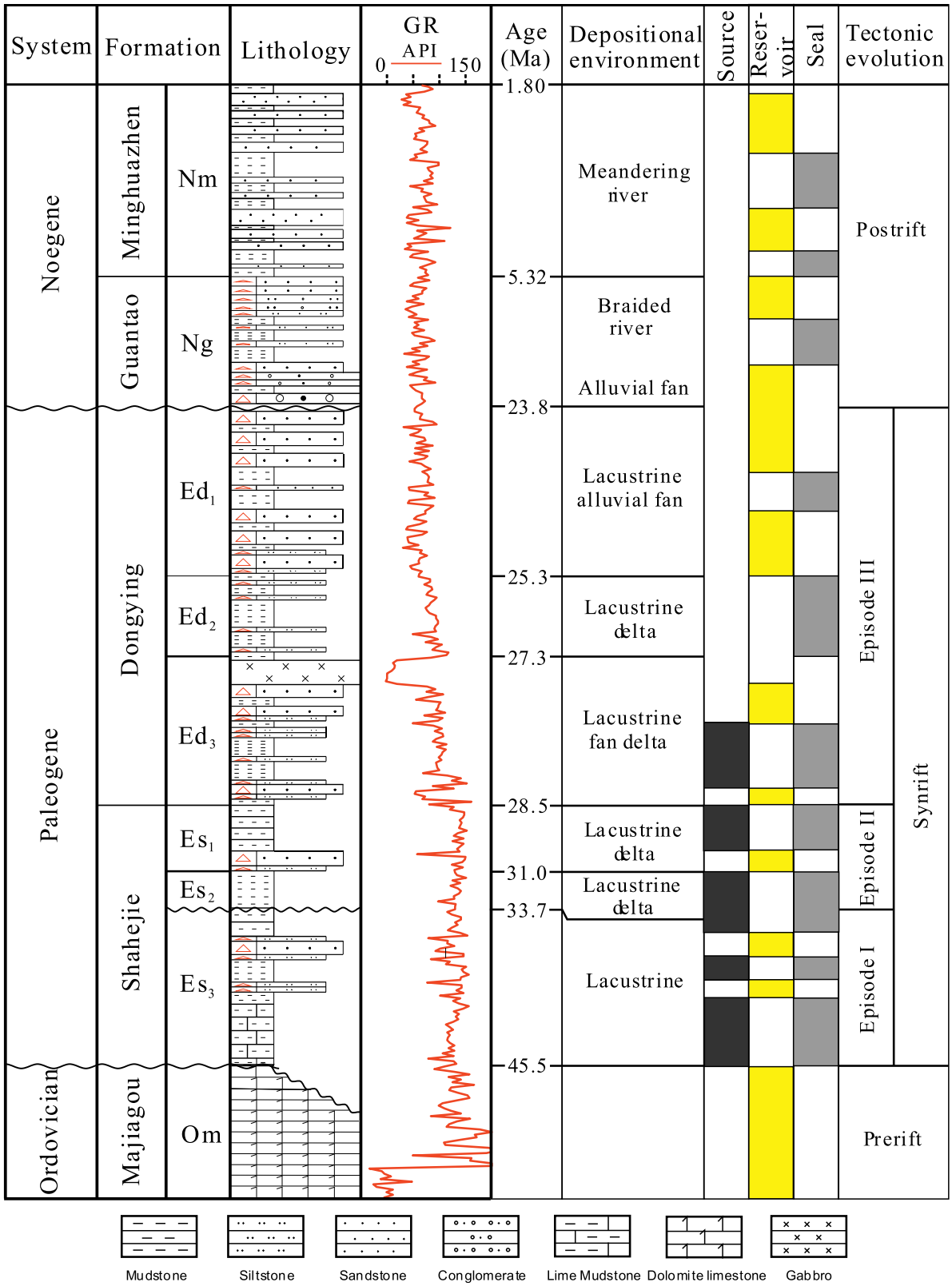

Figure 3. Stratigraphic column, petroleum system, and tectonic evolution of the Nanpu sag (modified from Dong et al., 2010; Guo et al., 2013; Chen et al., 2016). GR = natural gamma-ray logging.

Table 1. Natural Gas Component Contents in the Different Gas Layers in the Nanpu Sag

Well	Depth, m	Formation	C_1, %	N_2, %	CO_2, %	C_{2+}, %	C_1/C_{1+}
N38-10	1778.0	Nm	77.70	6.09	1.89	9.55	0.89
NP1	1819.6	Nm	88.21	0.88	0.15	1.55	0.98
N21	1643.1	Nm	77.58	0.73	4.50	12.16	0.86
L103-1	1804.7	Nm	82.33	1.52	–	8.18	0.91
N13	1353.3	Nm	95.40	3.36	0.98	0.00	1.00
NP11-C9-X205	1669.7	Nm	93.26	5.23	0.19	0.45	1.00
NP1-29	2253.7	Ng	78.36	1.33	1.17	7.27	0.92
M28-26	2049.3	Ng	92.87	1.48	0.28	2.71	0.97
NP1-3	2342.1	Ng	77.53	0.54	0.57	9.70	0.89
NP1-3	2342.1	Ng	78.26	0.72	0.52	8.75	0.90
NP1-15	2188.4	Ng	63.04	2.00	0.07	16.66	0.79
NP1-15	2188.4	Ng	59.25	0.48	0.10	20.69	0.74
LPN1	2362.3	Ng	74.59	0.00	1.92	1.03	0.99
LPN1	2217.9	Ng	72.87	0.00	0.72	3.18	0.96
NP1-22	2749.0	Ng	55.26	1.05	1.09	29.17	0.65
NP1-3	2342.1	Ng	60.75	3.85	0.65	17.18	0.78
NP2-3	2564.6	Ed_1	79.91	0.00	0.13	6.69	0.92
NP2-3	2564.6	Ed_1	80.15	0.00	0.13	6.55	0.92
NP1-5	2741.0	Ed_1	62.28	0.63	2.25	16.04	0.80
NP1-5	2741.0	Ed_1	68.31	0.50	1.91	13.37	0.84
NP1-2	2341.0	Ed_1	84.57	0.86	0.33	7.18	0.92
NP1-3	2646.5	Ed_1	81.96	0.67	1.05	6.39	0.93
LPN1	2506.5	Ed_1	74.59	0.00	1.92	1.03	0.99
M24X2	2701.7	Ed_2	91.58	–	1.90	2.50	0.97
M24X1	2645.8	Ed_2	91.39	0.43	0.74	2.94	0.97
M11	2516.8	Ed_2	93.07	1.13	0.40	1.74	0.98
M8x1	2369.0	Ed_2	84.19	1.08	0.46	6.93	0.92
B28	3169.5	Ed_2	91.46	1.40	0.27	2.48	0.97
B10	3132.0	Ed_2	91.48	0.87	0.44	3.00	0.97
M8X1	2332.8	Ed_2	89.12	3.74	–	2.47	0.97
B6X1	3073.6	Ed_2	85.06	1.50	1.60	5.30	0.94
G25X1	3302.7	Ed_2	85.02	1.18	2.44	11.13	0.88
Jh1X1	3526.4	Ed_3	86.16	1.88	1.09	5.32	0.94
B2	3551.8	Ed_3	81.92	1.97	0.29	8.25	0.91
B2	3551.8	Ed_3	81.70	1.93	1.40	7.56	0.92
M5	2366.5	Ed_3	87.26	0.95	3.98	2.37	0.97
B2	3551.8	Ed_3	82.31	1.51	0.69	8.01	0.91
B10	3641.1	Ed_3	89.44	1.18	0.95	2.99	0.97
G29	3089.5	Ed_3	91.43	0.52	0.73	2.18	0.98
G40	3186.2	Ed_3	93.43	0.15	0.05	2.74	0.97
B4	3841.6	Es_1	94.29	1.24	0.08	2.26	0.98
B12-1	4269.1	Es_1	53.59	0.00	–	23.43	0.70
PG1	3269.7	Es_1	84.64	0.47	2.38	4.37	0.95
G20	3821.0	Es_1	90.70	0.80	0.97	3.36	0.96
M7	2866.9	Es_1	78.45	4.11	0.30	8.64	0.90
G25X1	3960.3	Es_1	85.14	1.58	1.36	11.86	0.88

(*continued*)

Table 1. Continued

Well	Depth, m	Formation	C_1, %	N_2, %	CO_2, %	C_{2+}, %	C_1/C_{1+}
G10	3127.1	Es_3	93.88	0.74	0.24	2.48	0.97
G16	3769.5	Es_3	76.30	1.46	–	13.66	0.85
L13X1	3215.4	Es_3	68.37	1.59	–	15.92	0.81
L15-15	2598.8	Es_3	68.07	2.19	–	15.63	0.81
L17-17	3233.4	Es_3	77.78	5.33	0.08	7.97	0.91
G12	3585.7	Es_3	67.01	0.86	0.33	22.55	0.75
L15-15	2598.8	Es_3	75.76	2.64	–	10.72	0.88
L13	3230.9	Es_3	62.24	1.95	0.31	21.81	0.74
G16	3814.0	Es_3	78.31	1.29	–	12.39	0.86
L13-13	3116.8	Es_3	71.05	1.34	0.19	16.12	0.82
L11-12	3130.5	Es_3	62.67	2.51	–	23.10	0.73
L1	2578.5	Es_3	72.07	1.75	0.01	18.13	0.80

Abbreviations: – = not applicable; Ed_1 = first member of the Dongying Formation; Ed_2 = second member of the Dongying Formation; Ed_3 = third member of the Dongying Formation; Es_1 = first member of the Shahejie Formation; Es_3 = third member of the Shahejie Formation; Ng = Neogene Guantao Formation; Nm = Neogene Minghuazhen Formation.

30°C to 90°C at 15°C /min, and eventually from 90°C to 180°C at 6°C /min. Peak areas were integrated, and mole percent of the hydrocarbons was calculated. The precision of the analysis was ±5%.

A total of 116 samples were obtained, including 11 crude oil, 44 oil-bearing sandstone samples, and 61 shale samples. The typical shale and oil-bearing sandstone samples are shown in Figure 4. The 72 (11 oil-bearing sandstone samples and 61 shale samples) powdered samples (80–100 g) were extracted for 72 hr using a Soxhelt apparatus with chloroform as the solvent to obtain the extract (bitumen). The fraction separation of the bitumen for all (116) samples was performed using conventional column chromatography. The bitumen was dissolved in excess petroleum ether for 24 hr and filtered to obtain precipitable asphaltenes. The soluble components were separated by conventional column chromatography into saturated, aromatic hydrocarbon and resin fractions. The GC–mass spectrometry analysis for the saturated fractions was accomplished with a Thermo Fisher Scientific Finnigan Trace DSQ™ instrument

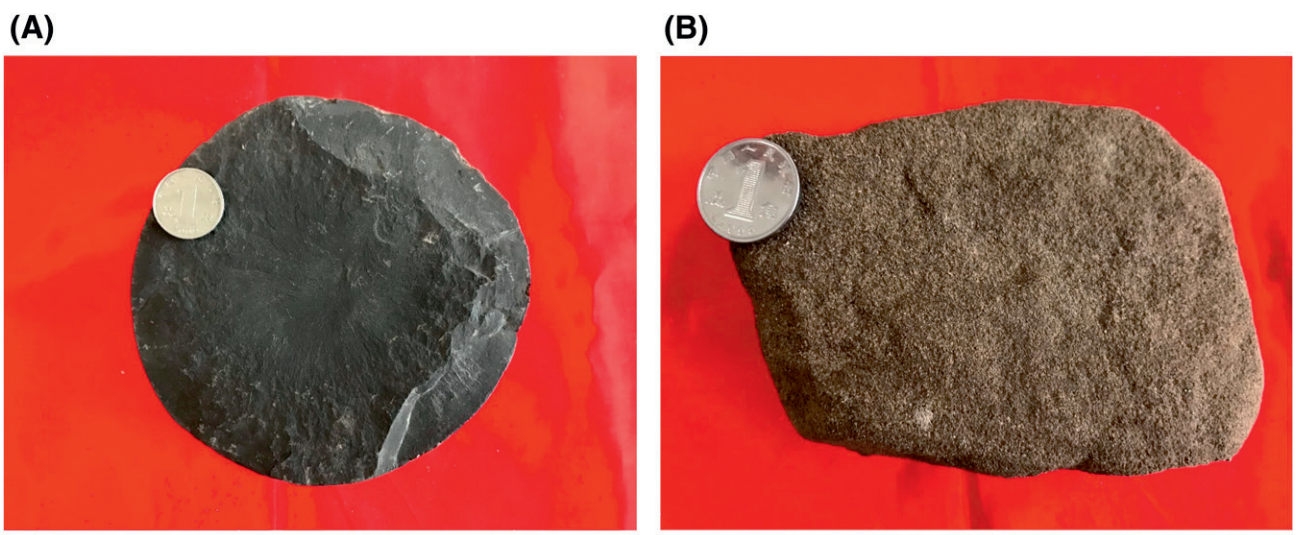

PG2, 4091.07 m, Ed_3, black shale sample.

NP1-5, 2717.40 m, Ed_1, oil-bearing sandstone sample.

Figure 4. Typical shale (A) and oil-bearing sandstone (B) samples in the Nanpu sag. Ed_1 = first member of the Dongying Formation; Ed_3 = third member of the Dongying Formation.

equipped with an HP-5MS fused silica column 60 m (196.8 ft) in length and 0.25 mm in diameter and coated with a thickness of 0.25 μm of silica gel film. The GC oven temperature was initially held at 50°C for 1 min and later programmed to 120°C at 20°C/min, 250°C at 4°C/min, and 310°C at 3°C/min and was finally held at 310°C for 30 min.

HYDROCARBON DISTRIBUTION

The relationships among source rock, oil-bearing layers, and cap rocks display three source-reservoir-cap assemblages (Figures 2, 5): (1) new-bed generation and old-bed preservation (NG-OP), (2) self-generation and self-preservation (SG-SP), and (3) old-bed generation and new-bed preservation (OG-NP). The NG-OP assemblage means that the discovered oil and gas are generated in new strata but accumulated in relatively old strata, the SG-SP assemblage means the reservoir and the source rock are in the same layers, and the OG-NP assemblage means the discovered oil and gas are generated in old strata but accumulated in relatively new strata. The NG-OP assemblage exists in the nos. 1–4 SBs. Most of the oil and gas were distributed in the Ordovician strata at the base of the main source rock (Shahejie Formation) that is also the cap rock (Figure 5). The SG-SP assemblage is in the Gaoshangpu and Liuzan SBs. The discovered oil and gas are chiefly distributed in the Ed_3 to Es_3. There appears to be frequent interbedding of multiple source rocks and reservoirs. In other SBs, the SG-SP assemblage is not very developed (Figure 5). The OG-NP assemblage exists in the Beipu, Laoyemiao, Gaoshangpu, Liuzan, and nos. 1–2 SBs (Figure 5). The discovered oil and gas are entirely generated and migrated from the Ed_3 to Es_3 source rocks. Most SBs contain oil, which is mainly distributed in the Ed_2, Ed_1, Ng, and Nm, especially in the Ng and Ed_1, but the oil and gas in the Nm is chiefly onshore (Figure 5).

Formation testing results show that the oil layers and gas layers differ in their vertical distribution (Figure 6). The oil layers are mainly distributed in the upper formations, such as the Nm, Ng, and Ed_1. In addition, several of them are distributed in the Es_3 in the Liuzan and Gaoshangpu SBs (Figure 6A). Most of the gas layers are distributed in the Ed_3 followed by the Ed_2 and Ed_1, with few being found in the upper or lower formations (Figure 6B). All of the tested oil and gas layers are at depths greater than 1500 m (>4920 ft). The gas layers are mainly distributed in the depth interval of 3000–4000 m (~9840–13,120 ft),

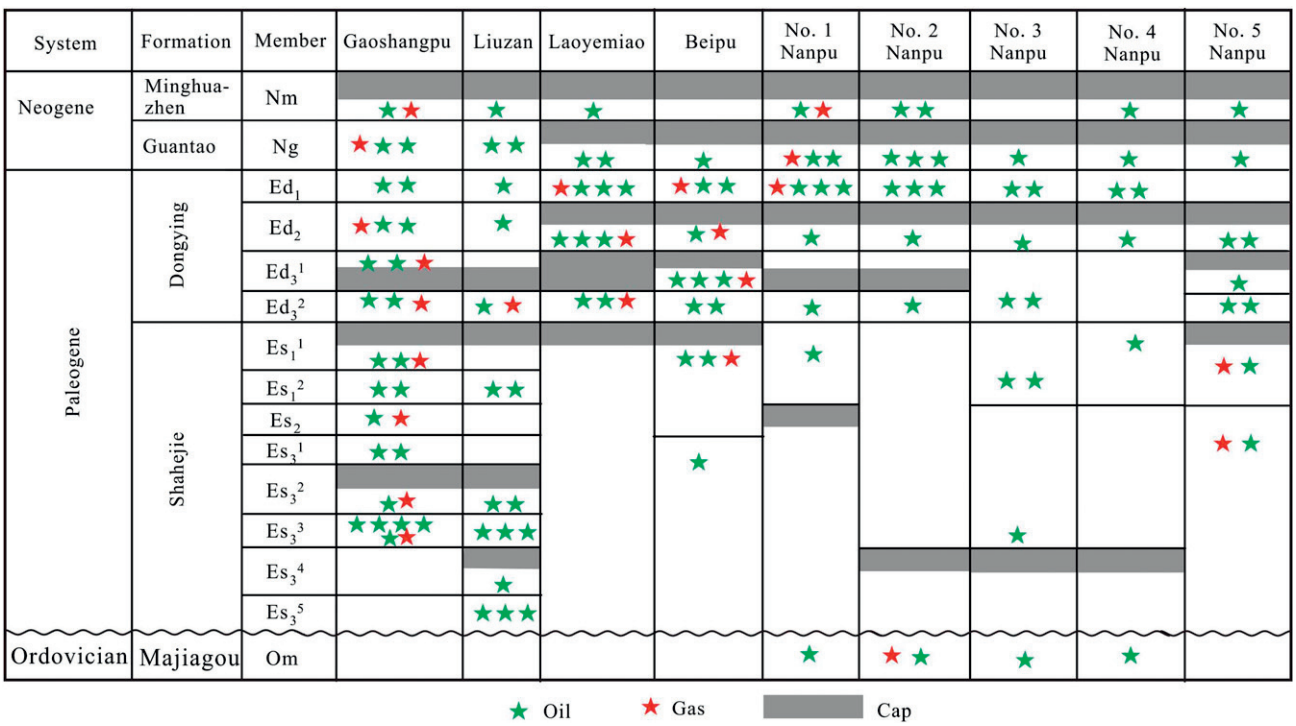

Figure 5. Reservoir-cap assemblage and the vertical distribution of the oil and gas in the different structural belts of the Nanpu sag.

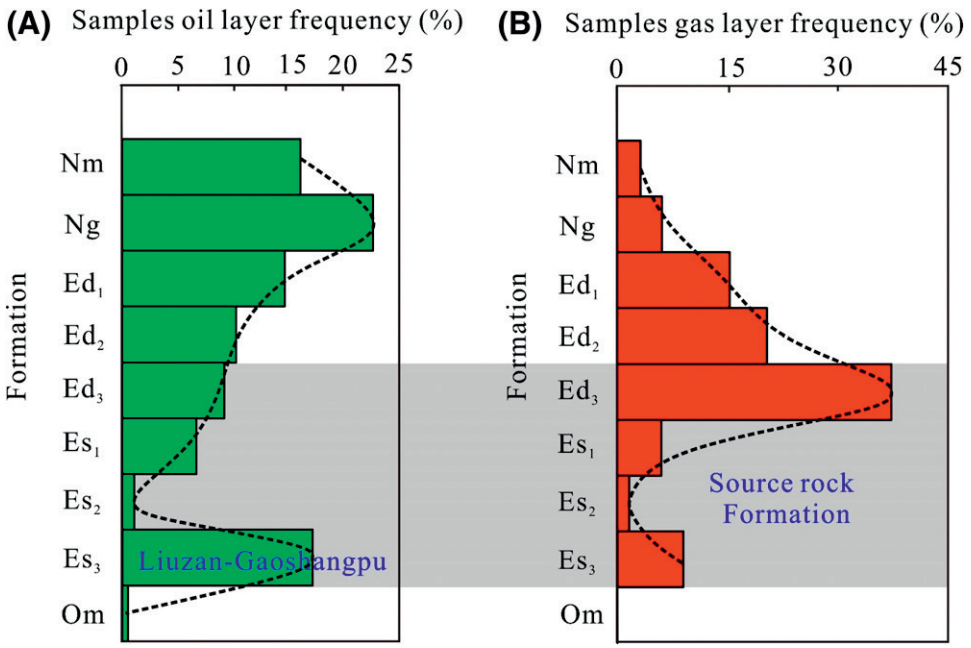

Figure 6. Distribution of the testing oil (A) and gas layers (B) in the different formations of the Nanpu sag. Ed_1 = first member of the Dongying Formation; Ed_2 = second member of the Dongying Formation; Ed_3 = third member of the Dongying Formation; Es_1 = first member of the Shahejie Formation; Es_2 = second member of the Shahejie Formation; Es_3 = third member of the Shahejie Formation; Ng = Neogene Guantao Formation; Nm = Neogene Minghuazhen Formation; Om = Ordovician Majiagou Formation.

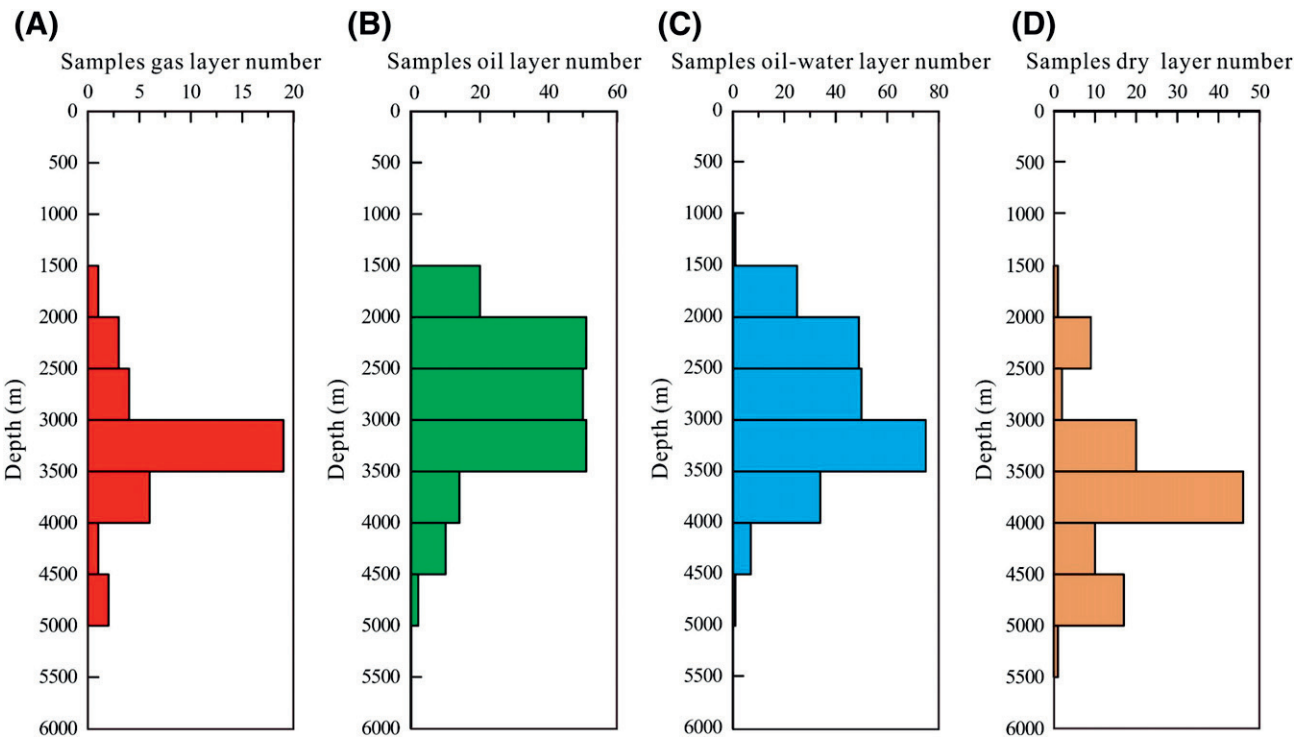

Figure 7. Distribution of the testing gas (A), oil (B), oil–water (C), and dry layers (D) versus depth in the Nanpu sag.

whereas the oil layers and oil–water layers are chiefly distributed between 2000 and 3500 m in depth (~6560–11,480 ft) (Figure 7A–C). The accumulation characteristics are different for the oil and gas layers. Additionally, the dry layers (dense reservoir not containing crude oil, gas, or formation water) are principally below 3000 m (9840 ft) in depth (Figure 7D). The discovered oil and gas fields are around the Linque, Liunan, and Caofeidian subsags with a ring-shaped distribution (Figure 8). The gas fields are considerably closer to the subsag center, and the oil fields are distributed farther to the edge of the subsag.

CHARACTERISTICS AND SOURCES OF HYDROCARBONS

Oil Density and Viscosity

In the Nanpu sag, the density and viscosity values of the crude oil samples cover a wide range. However, there are several trends in the different SBs (Figure 9). Generally, most of the oil samples are light-medium oil, but there is also heavy oil discovered mainly in the Gaoshangpu and Liuzan SBs (Figure 9).

The density of the lightest oil is less than 0.87 g/cm^3, and the viscosity is less than 40 mPa·s (Figure 9). Over a depth of 2200 m (7216 ft), the density and viscosity values of the crude oils increase as the buried depth decreases, ranging from 0.87 to 0.97 g/cm^3 and from 40 to 600 mPa·s (even greater than 1000 mPa·s, locally), respectively. The heavy or viscous oil is mainly distributed in the onshore Liuzan and Gaoshangpu SBs, whereas the crude oil in the Laoyemiao SB is medium light (Figure 10A, B). The density and viscosity of the crude oil in the Beipu and offshore areas have relatively low values, which are lower than 0.83 g/cm^3 and 10 mPa·s, respectively (Figure 10A, B). In general, the heavy crude oil is the product of secondary actions, such as biodegradation, oxidation, and dispersion of the light fraction (Killops and Al-Juboori, 1990; Wenger et al., 2002; Head et al., 2003). In the 2700–3000 m (~8856–9840 ft)

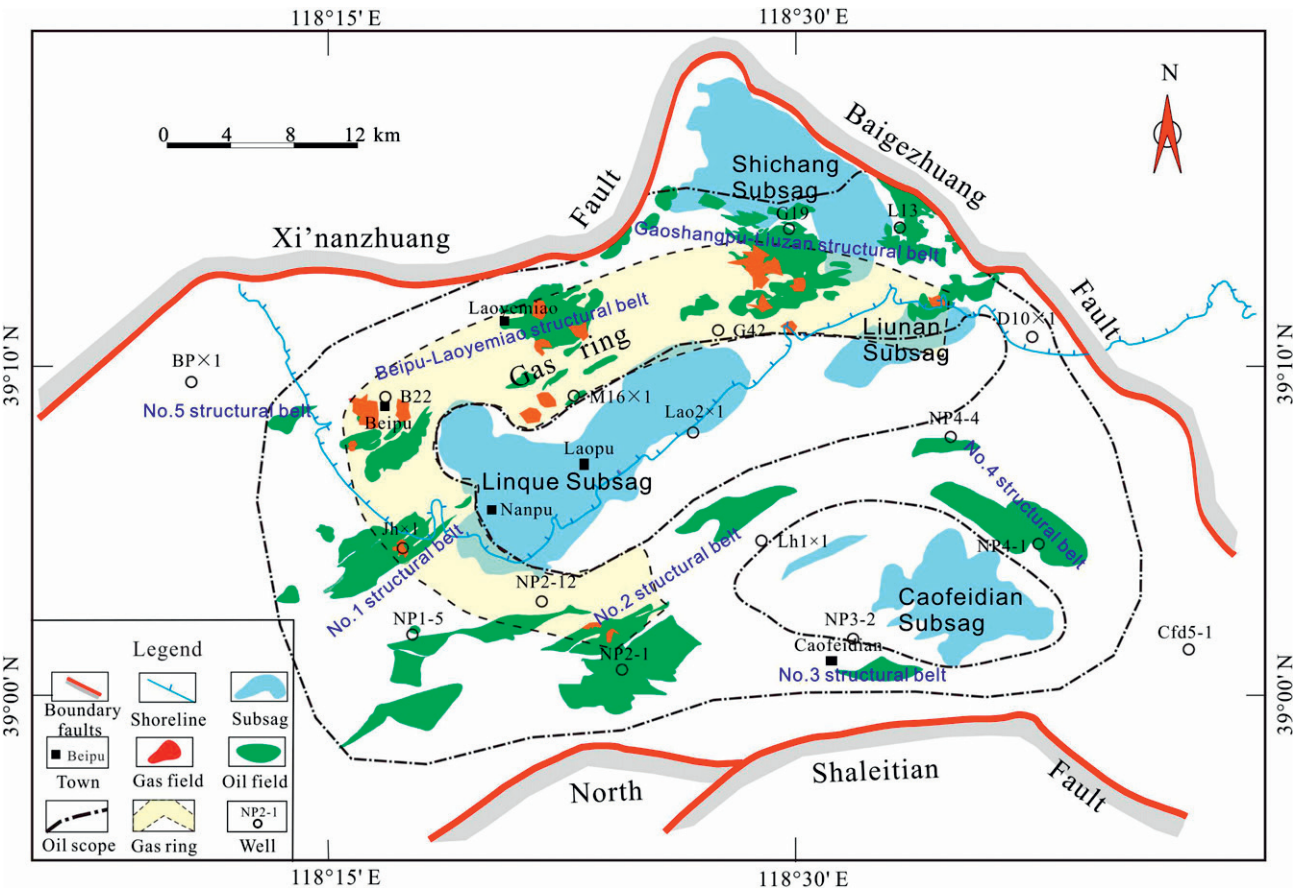

Figure 8. Distribution of the oil and gas fields in the Nanpu sag showing an oil scope and gas ring around the hydrocarbon generation subsag.

depth range of the Liuzan SB, a fraction of crude oil with a high density and viscosity is related to the uplift after the early oil accumulation and a second deep burial stage (Wang and Zheng, 2008).

Furthermore, the density and viscosity values of some crude oil samples are lower than 0.80 g/cm^3 and 1 mPa·s at a depth of 3250 m (10,660 ft), which are light oil in a condensate gas reservoir (Figure 10A, B). When the reservoirs are at a high temperature and high pressure in the deep basin, a lighter hydrocarbon mixture may exist in the gas phase (Pápay, 2003; Ayala et al., 2007; Liu et al., 2009). At the surface, the mixtures will divide into two phases: a liquid light oil (condensate oil) and gas. The density and viscosity values increase gradually as the buried depth or temperature and pressure decrease (Figure 10).

Oil Types and Sources

The biomarkers are good indicators for oil-source correlations. Because the normal alkanes and isoparaffins are considerably more readily affected by secondary alteration, the relatively stable sterane and terpane biomarkers better reflect such parameters as the depositional environment, organic matter source, and thermal maturity level (Wenger et al., 2002). Based on the sterane and terpane biomarker characteristics, the crude oils are divided into four types: A, B, C, and D (Table 2).

The type A oil contains a high content of 4-methyl-C_{30} sterane and a low content of gammacerane. For the type A oil, the contents of 4-methyl-C_{30} sterane are higher than the other oils. The gammacerane/C_{30} hopane, C_{27} 18α (H),22,29,30-trisnorneohopane/C_{27} 17α (H),22,29,30-trisnorhopane (Ts/Tm), and diasterane/regular sterane ratios range from 0.06 to 0.08, from 1.00 to 2.24, and from 0.10 to 0.12, respectively (Table 2). This finding indicates a fresh water lacustrine depositional setting. An approximately symmetrical V-shaped distribution pattern of C_{27}, C_{28}, and C_{29}ααα(20R) steranes (where R is right-handed stereo configuration) indicates contribution of both aquatic organisms and terrestrial higher plants (Huang and Meinschein, 1979; Volkman et al., 1998; Köhler and Clausing, 2000; Adegoke et al., 2014) (Figure 11). The higher content of C_{27}, C_{28}, and C_{29} αββ steranes shows that the maturity level of the source rock is elevated. Type A oil is mainly discovered in the Es_3 in the Liuzan and Gaoshangpu SBs (Figure 5). The oil-source correlation results indicate that the type A oil is chiefly derived from the Es_3 source rock in the Shichang subsag (Figure 11).

Type B oil displays lower 4-methyl-C_{30} sterane and gammacerane abundances than the type A oil. This oil type contains a slightly higher content of Ts than Tm (Ts/Tm > 1) and a lower content of pregnanes. The gammacerane/C_{30} hopane, Ts/Tm, and diasterane/regular sterane ratios range from 0.06 to 0.15, from 1.14 to 1.58, and from 0.15 to 0.17, respectively (Table 2). The C_{27}, C_{28}, and C_{29}ααα(20R) steranes display an L-shaped distribution (Figure 12). This finding indicates that the depositional environment of the type B oil was also freshwater lacustrine. The organic matter was mainly derived from lower aquatic organisms (Köhler and Clausing, 2000; Adegoke et al., 2014). Type B oil is derived from the Ed_3 source rock of the Gaoshangpu and Liunan subsags (Figure 12).

Type C oil contains a very low content of 4-methyl-C_{30} sterane and gammacerane. The gammacerane/C_{30} hopane, Ts/Tm, and diasterane/regular sterane ratios range from 0.06 to 0.13, from 1.00 to 1.50, and from 0.11 to 0.19, respectively (Table 2). The distribution of the C_{27}, C_{28}, and C_{29}ααα(20R) steranes is L-shaped (Figure 13). This finding indicates that the type C oil was derived from fewer aquatic organisms in a depositional environment with a low water salinity. In

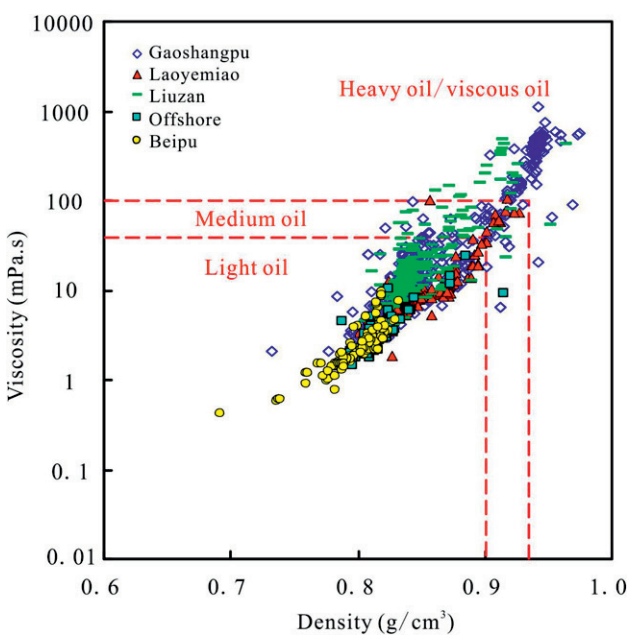

Figure 9. Relationship between the density and viscosity for the crude oil in the Nanpu sag.

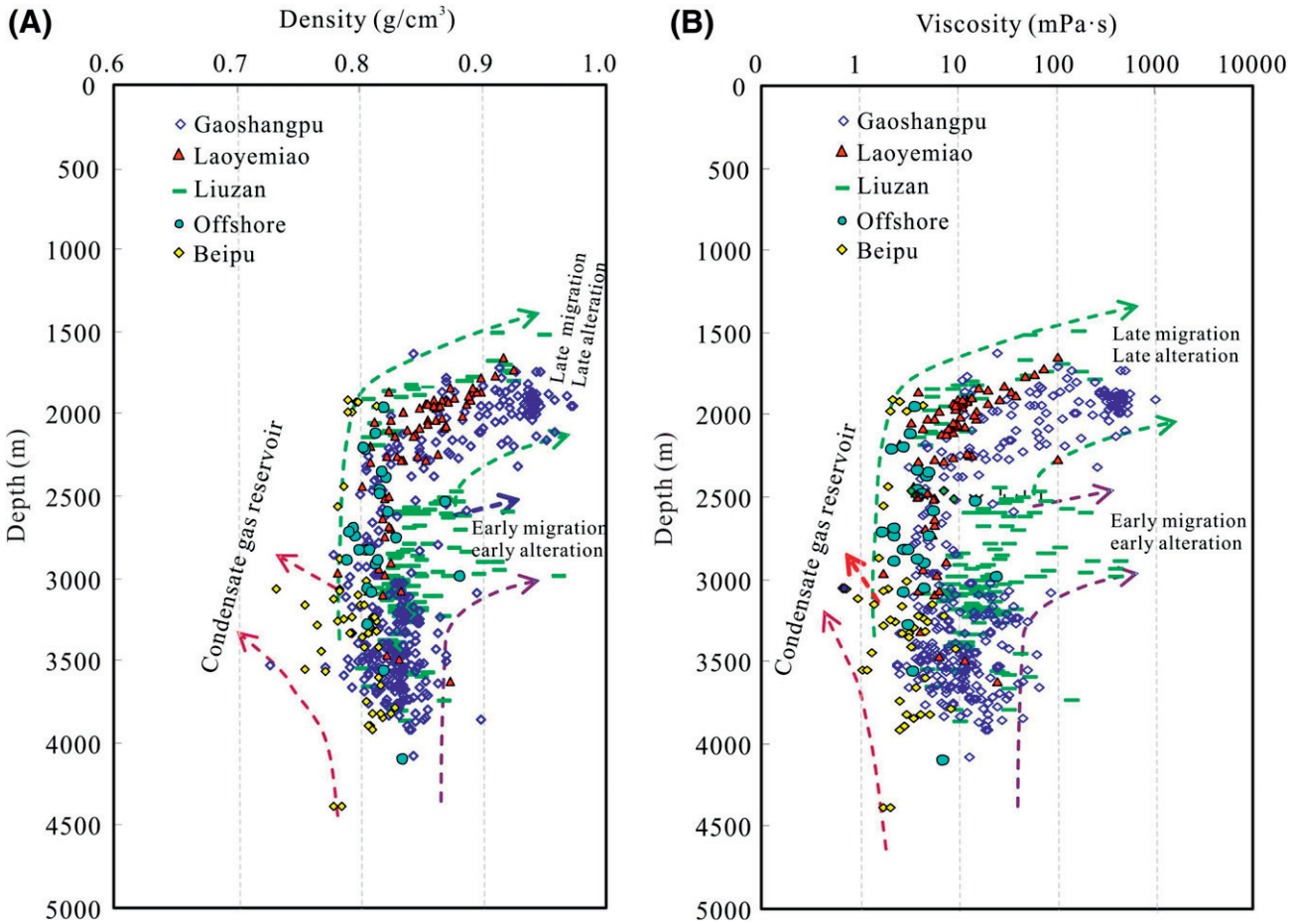

Figure 10. Scatter plots of the density (A) and viscosity (B) versus depth in the Nanpu sag.

addition, type C oil samples range from low to middle maturity (Table 2) (Köhler and Clausing, 2000). The detailed oil-source correlation shows that the type C oil is from the Ed_3 and Es_1 source rocks, which have similar geochemical characteristics (Figure 13).

Type D oil contains a relatively high content of gammacerane and a low content of 4-methyl-C_{30} sterane. The gammacerane/C_{30} hopane, Ts/Tm, and diasterane/regular sterane ratios range from 0.16 to 0.47, from 1.00 to 1.20, and from 0.09 to 0.15, respectively (Table 2). This result indicates that the depositional environment of the type D oil is saline lacustrine. The type D oil is an L-shaped distribution pattern of C_{27}, C_{28}, and $C_{29}\alpha\alpha\alpha$(20R) steranes, which was mainly derived from fewer aquatic organisms (Volkman et al., 1998; Köhler and Clausing, 2000; Adegoke et al., 2014). The type D oil is closely related to the Es_3 source rock with a relatively lower maturity (Figure 14).

As is depicted in Figure 15, there are different distributions for different types of crude oils. The type A oil mainly occurs in the reservoirs of the Gaoshangpu and Liuzan SBs around the Shichang subsag. Additionally, the type B oil is distributed along the Laoyemiao, south of the Gaoshangpu and Liuzan SB. The type C oil mainly occurs around the Beipu and the nos. 1–4 SBs. Finally, the type D oil is principally distributed along the Beipu and nos. 1, 2, and 5 SBs. It should be noted that the type C and D oils have an overlapping distribution zone in the Beipu and the nos. 1 and 2 SBs, indicating that in this area, the oils may be derived from multiple source rocks (Figure 15).

Natural Gas Characteristics and Source

In the Nanpu sag, the natural gas is mainly dissolved gas in oil, but there is also some free gas. Based on the formation test results, the gas-to-oil ratios of the tested

Table 2. Comparison for the Characteristics of the Four Different Oils in the Nanpu Sag

Parameters	Type A	Type B	Type C	Type D
C_{27}, C_{28}, and C_{29} sterane	V-shaped	L-shaped	L-shaped	L-shaped
4-Methyl-C_{30} sterane	Highest	High	Low	Lower
Gammacerane	Lower	Low	Low	High
Gammacerane/C_{30} hopane	0.06–0.08	0.06–0.15	0.16–0.13	0.16–0.47
Ts/Tm	1.00–2.24	1.14–1.58	1.00–1.50	1.00–1.20
Diasterane/regular sterane	0.10–0.12	0.15–0.17	0.11–0.19	0.09–0.15
Maturity	High	Middle to high	Low to middle	Low to middle
Reduction or oxidation	Weak reduction	Weak reduction	Weak reduction	Weak reduction
Salinity	Lower	Low	Low	High
Source of the organic matter	Aquatic organisms and terrestrial higher plants	Aquatic organisms	Aquatic organisms	Aquatic organisms
Source rock	Es_3 of the Shichang subsag	Ed_3 of the Gaoshangpu and Liunan subsags	Ed_3 to Es_1 of the Beipu and offshore	Es_3 of the offshore
Distribution of the crude oil	Es_3 of the Gaoshangpu and Liuzan	Nm to Ed_3 of the onshore	Nm to Ed_3 of the offshore	Nm to Ed_3 of the offshore

Abbreviations: Ed_3 = third member of the Dongying Formation; Es_1 = first member of the Shahejie Formation; Es_3 = third member of the Shahejie Formation; Nm = Neogene Minghuazhen Formation; Ts/Tm = C_{27} 18α (H),22,29,30-trisnorneohopane/C_{27} 17α (H),22,29,30-trisnorhopane.

zones display a wide range in the different SBs (Figure 16; Table 3). The gas-to-oil ratios of several onshore areas (such as Liuzan, Gaoshangpu, and Laoyemiao) show a decreasing trend as the buried depth decreases (Figure 16A–C). However, the gas-to-oil ratios shows little change in the offshore areas (Figure 16D). This indicates that there are abundant solution gases in both the onshore and offshore areas of the Nanpu sag.

The natural gas in the Nanpu sag mainly consists of methane with a minor amount of nonhydrocarbons (Table 1). Methane contents range from 59.25% to 95.40% (mean = 79.57%) (Table 1). The contents of heavy hydrocarbon (C_{2+}) range from 0.00% to 29.17% (mean = 8.93%). The nonhydrocarbons mainly consist of nitrogen and carbon dioxide. The contents of the carbon dioxide range from 0.00% to 4.50% (mean = 0.94%), most being less than 3.00%. The nitrogen content ranges from 0.00% to 6.09% (mean = 1.49%) (Table 1).

The gas dryness coefficient (C_1/C_{1+}) values range from 0.65 to 1.00 (mean = 0.90), with a small population greater than 0.95. These values indicate that the natural gas samples are mainly wet gas (Clayton, 1991; Saberi and Rabbani, 2015). Dry gas is mainly distributed in the upper Nm and Ng (Figure 17A). The C_1/C_{1+} ratio increases as the depth decreases in Ed_2, Ed_1, Ng, and Nm. This shows that there is vertical migration differentiation of the natural gas (Figure 17A).

In the Ed_3, Es_1, and Es_3 source rocks, the C_1/C_{1+} ratio does not show a regular variation with the burial depth (Figure 17B). The wet gas and dry gas are distributed in both the deep and shallow formations, but the wet gas is more abundant. The natural gas with the lower C_1/C_{1+} ratio is chiefly distributed at the depth interval between 3100 and 4200 m (~10,168–13,776 ft), corresponding to the peak oil generation (Figure 17C). This indicates that the natural gas dryness in the source rock layers is strongly controlled by thermal maturity.

SOURCE ROCK CONTROL ON THE HYDROCARBON DISTRIBUTION

In Figure 18, the biomarker parameters Ts/Tm and $\alpha\alpha\alpha$-S/(S + R)-C_{29} sterane (where S is left-handed

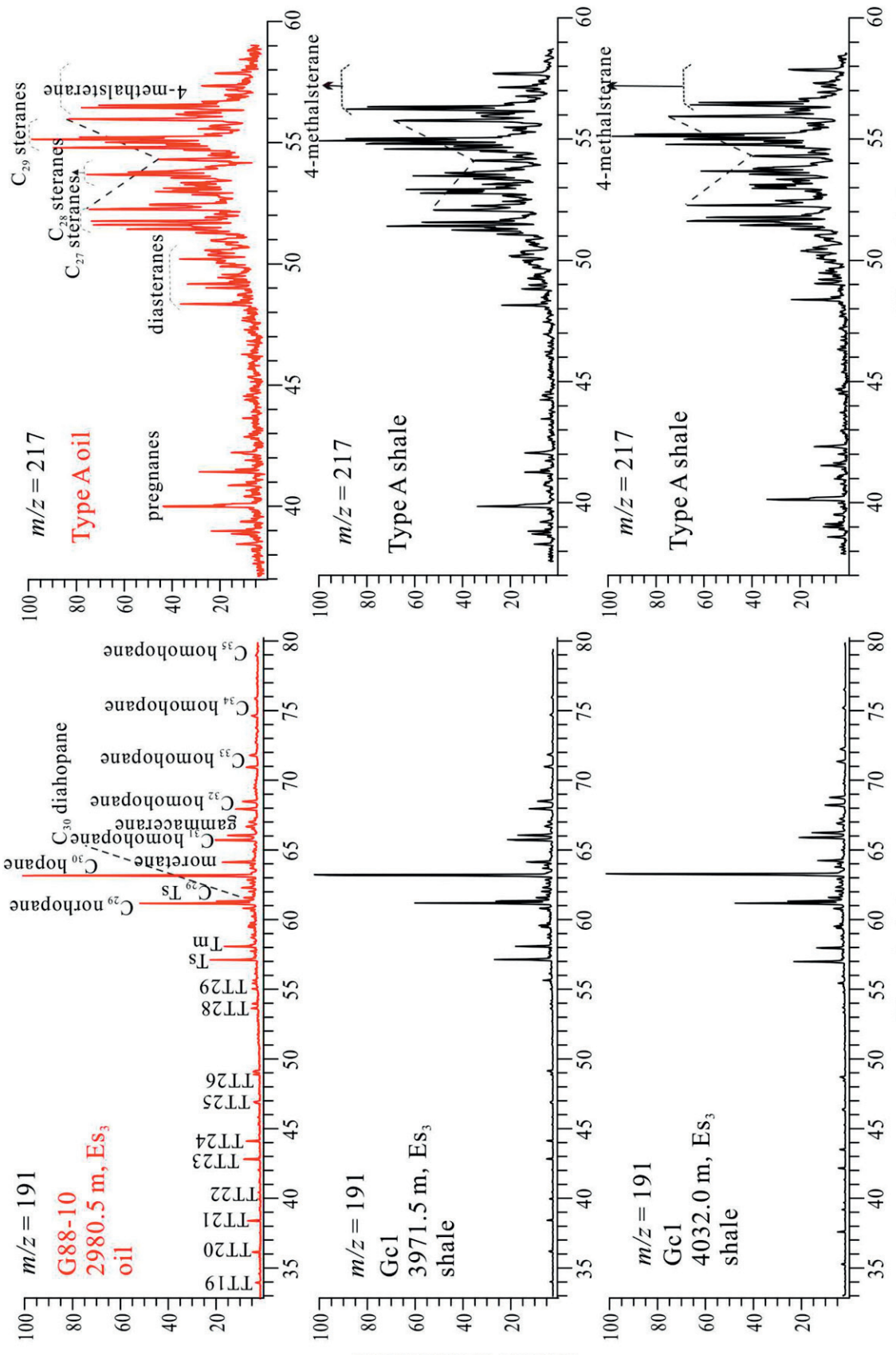

Figure 11. Terpane (mass-to-charge ratio [*m/z*] = 191) and sterane (*m/z* = 217) fragmentograms for type A oils and shales in the Nanpu sag. Es_3 = third member of the Shahejie Formation; Tm = C_{27} 17α (H),22,29,30-trisnorhopane; Ts = C_{27} 18α (H),22,29,30-trisnorneohopane; TT = tricyclic terpane.

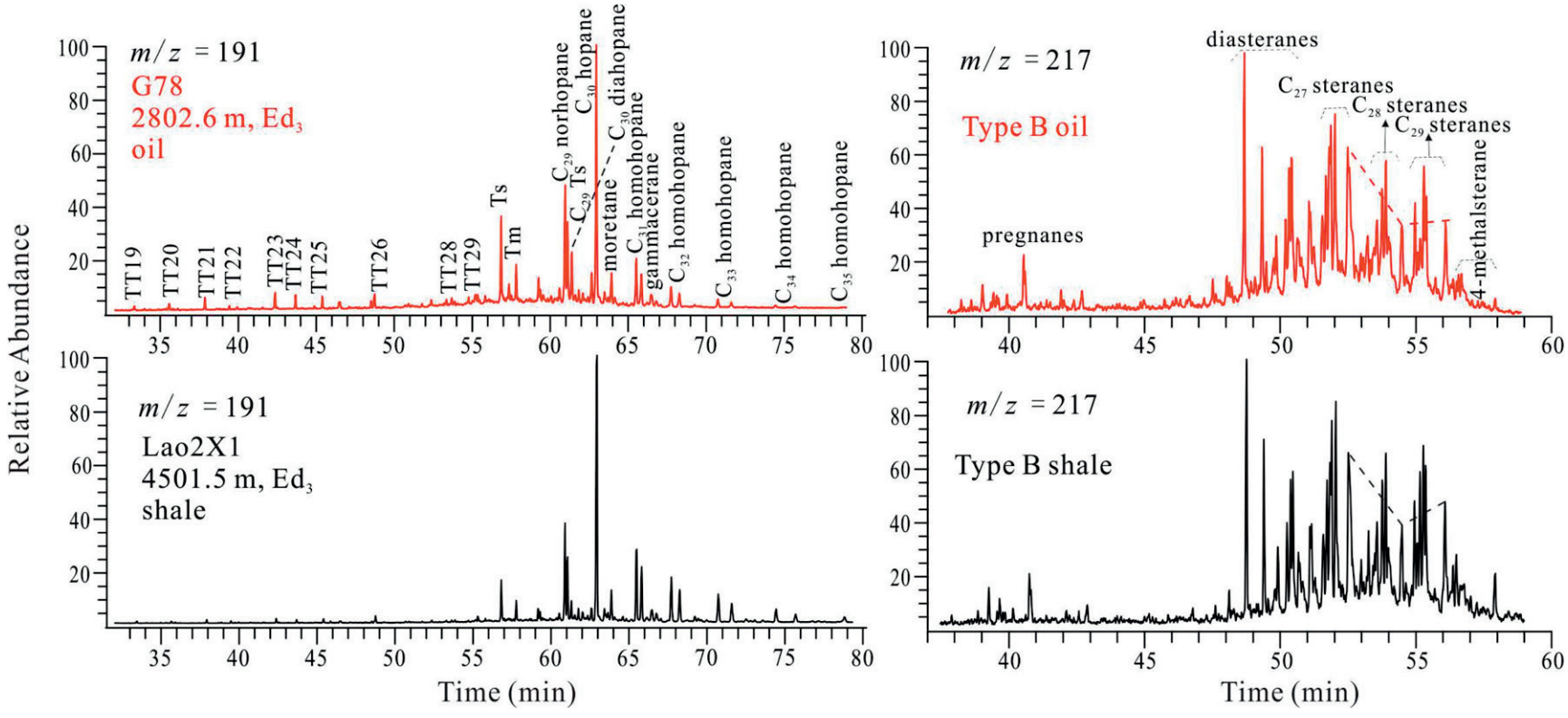

Figure 12. Terpane (mass-to-charge ratio [*m/z*] = 191) and sterane (*m/z* = 217) fragmentograms for type B oils and shales in the Nanpu sag. Ed_3 = third member of the Dongying Formation; Tm = C_{27} 17α (H),22,29,30-trisnorhopane; Ts = C_{27} 18α (H),22,29,30-trisnorneohopane; TT = tricyclic terpane.

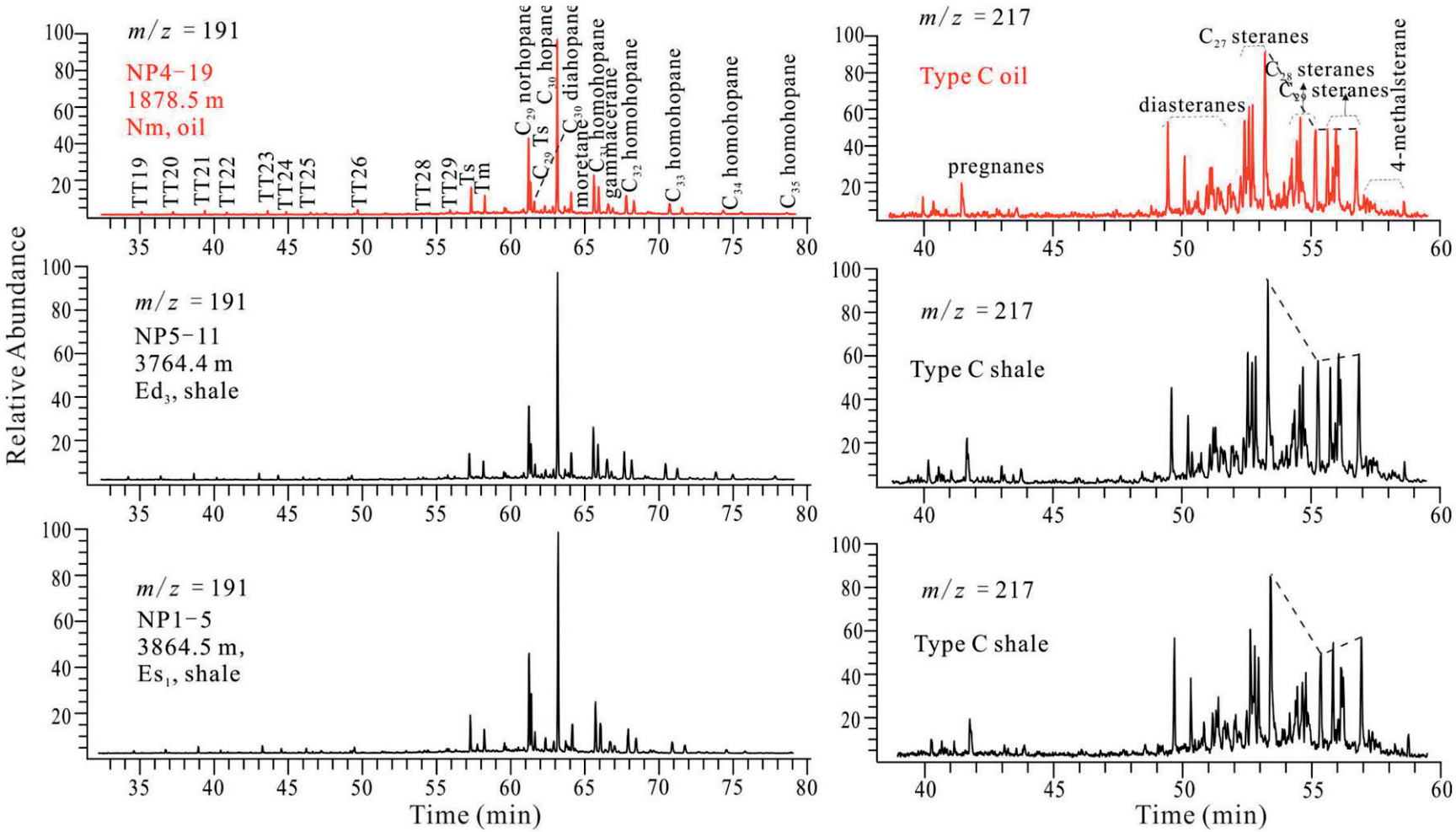

Figure 13. Terpane (mass-to-charge ratio [*m/z*] = 191) and sterane (*m/z* = 217) fragmentograms for type C oils and shales in the Nanpu sag. Ed_3 = third member of the Dongying Formation; Es_3 = third member of the Shahejie Formation; Tm = C_{27} 17α (H),22,29,30-trisnorhopane; Ts = C_{27} 18α (H),22,29,30-trisnorneohopane; TT = tricyclic terpane.

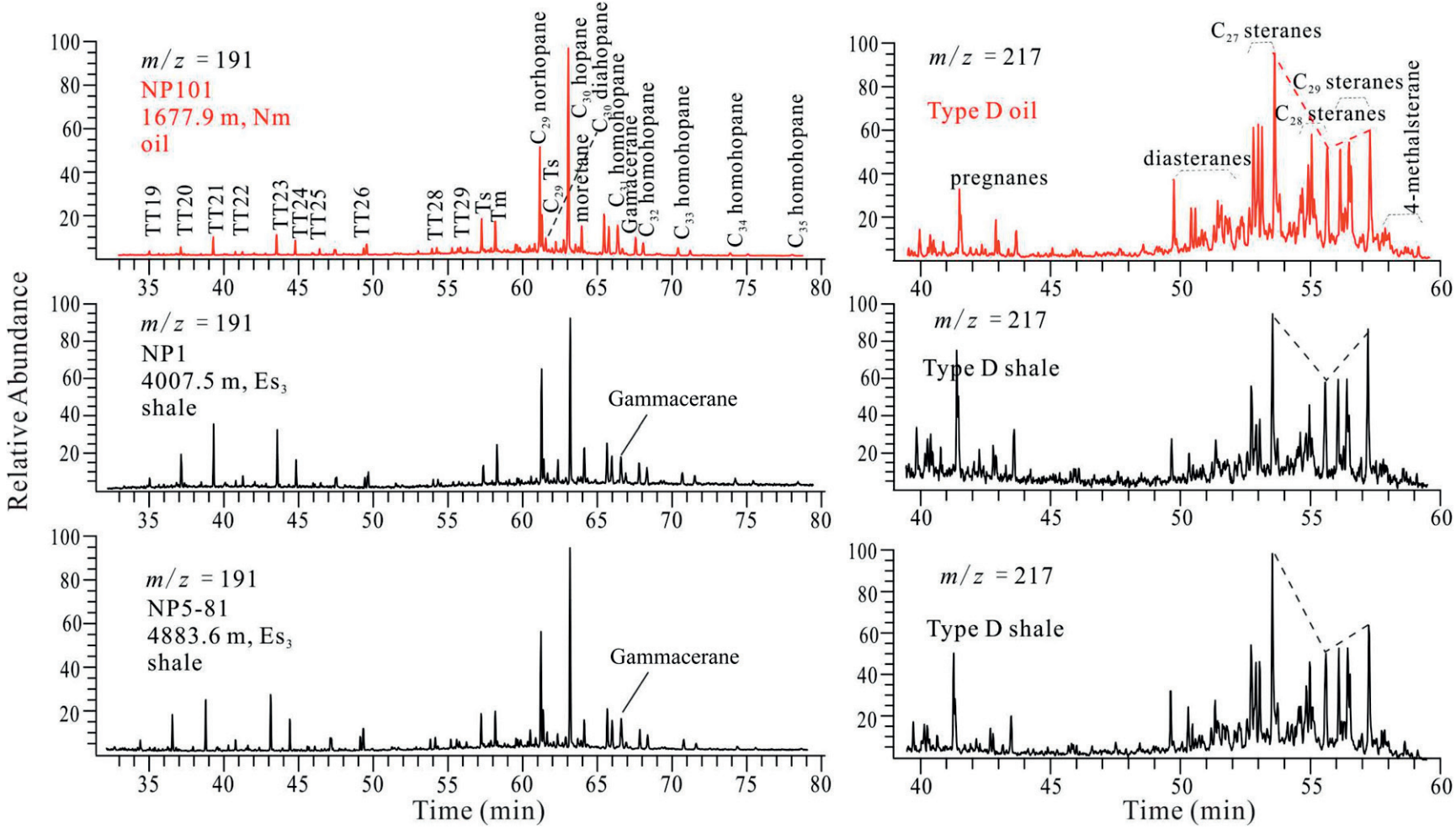

Figure 14. Terpane (mass-to-charge ratio [*m/z*] = 191) and sterane (*m/z* = 217) fragmentograms for type D oils and shales in the Nanpu sag. Es_3 = third member of the Shahejie Formation; Tm = C_{27} 17α (H),22,29,30-trisnorhopane; Ts = C_{27} 18α (H),22,29,30-trisnorneohopane; TT = tricyclic terpane.

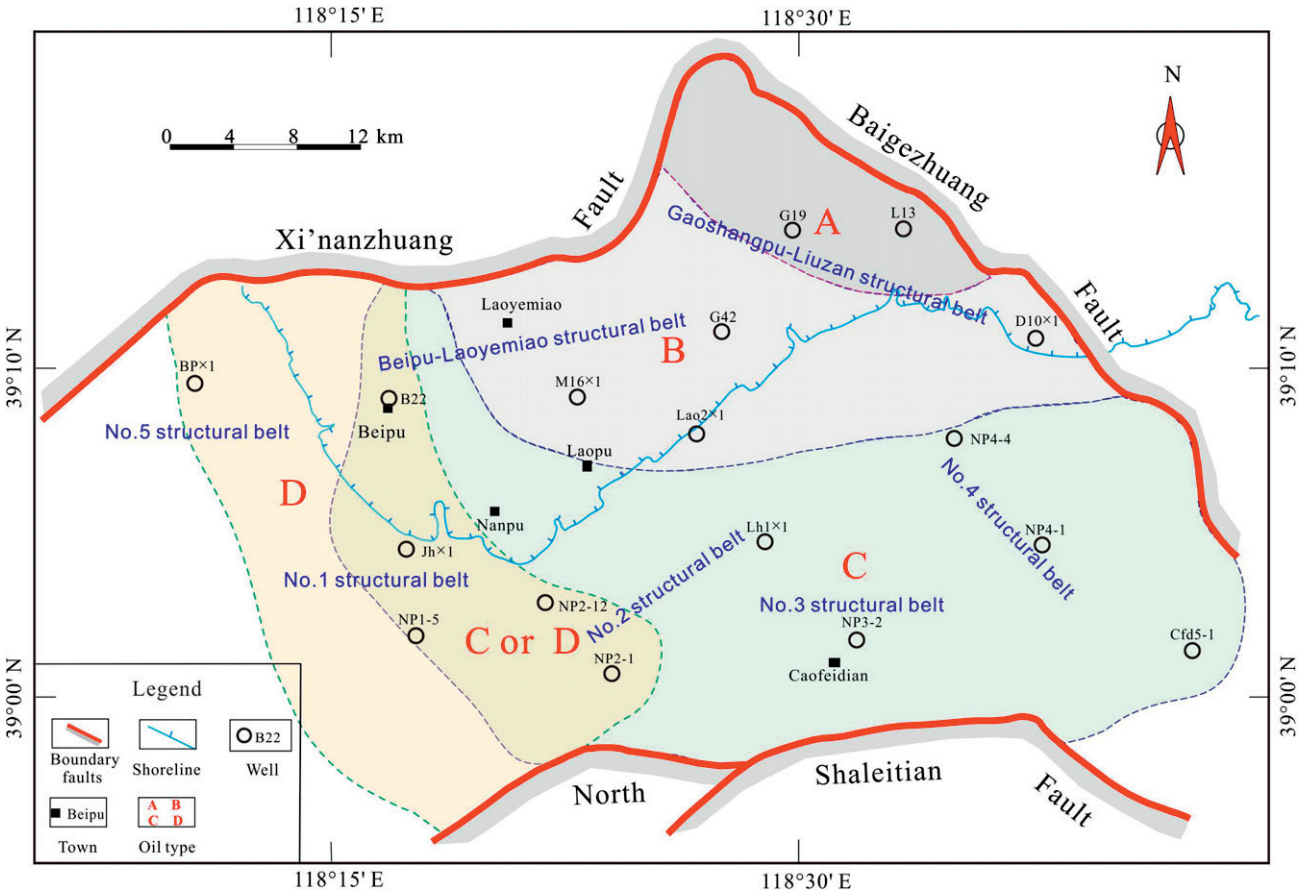

Figure 15. Distribution map of the four different oils in the Nanpu sag.

stereo configuration) ratios of the crude oil from the different layers do not vary significantly as burial depth changes (Table 4). Additionally, the biomarker parameters of the crude oils are clearly higher than that of the source rocks at the shallow depth, showing that the shallow source rocks had no contribution to the accumulations. At the depth of approximately 3100 m (~10,168 ft), the biomarker parameters of the crude oils reached the source rocks' values (Figure 18A, B). This indicates that the source rocks are within the oil-generating window beyond a depth of 3100 m (10,168 ft) (Figure 17C). In addition, the crude oil has experienced obvious vertical migration from deep to shallow.

There are three-dimensional (3-D) seismic data and thousands of wells in the Nanpu sag. Isopachs of the Es_3, Es_1, and Ed_3 were obtained using the 3-D seismic data. A relationship between sedimentary facies and shale/stratum thickness ratio was established. And then, the source-rock thickness contour maps of the Es_3, Es_1, and Ed_3 are plotted using the statistical results of the dark shale thickness of the wells and seismic prediction (Figure 19). The oil and gas are mainly distributed in the areas with thicker source rock. In the northwest and southeast of the sag there are two depocenters, with the thickest being more than 600 m (1968 ft) (Figure 19A). The type A and D oils are mainly distributed in the west and northwest of the Es_3 source rock, respectively. This finding suggests that the type A and D oils are derived from the Es_3 source rock with a different maturity. The Es_3 is the major hydrocarbon source rock, making the greatest contribution to the oil and gas generation in the Nanpu sag, which is in agreement with the previous oil-source correlation results (Zheng et al., 2007a, b; Mei et al., 2009).

The Es_1 source rock is thinner than the Es_3 source rock, only approximately 300 m (~984 ft) at most, with the depocenter migrating to the southeast of the Nanpu sag. The type C oil, which is derived from the Es_1 source rock, is mainly distributed from the west to south in the southern

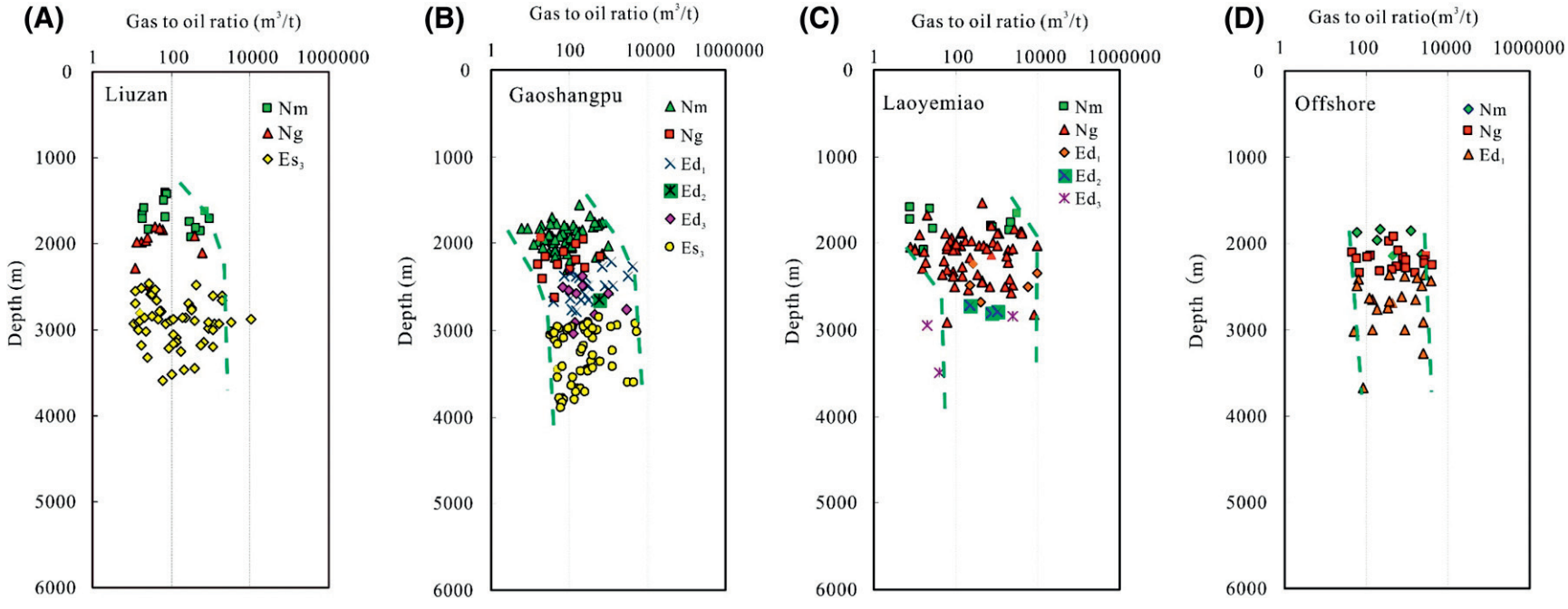

Figure 16. Scatter plots of the gas-to-oil ratio versus depth in the Liuzan (A), Gaoshangpu (B), Laoyemiao (C), and offshore structural belts in the Nanpu sag. Ed_1 = first member of the Dongying Formation; Ed_2 = second member of the Dongying Formation; Ed_3 = third member of the Dongying Formation; Es_3 = third member of the Shahejie Formation; Ng = Neogene Guantao Formation; Nm = Neogene Minghuazhen Formation.

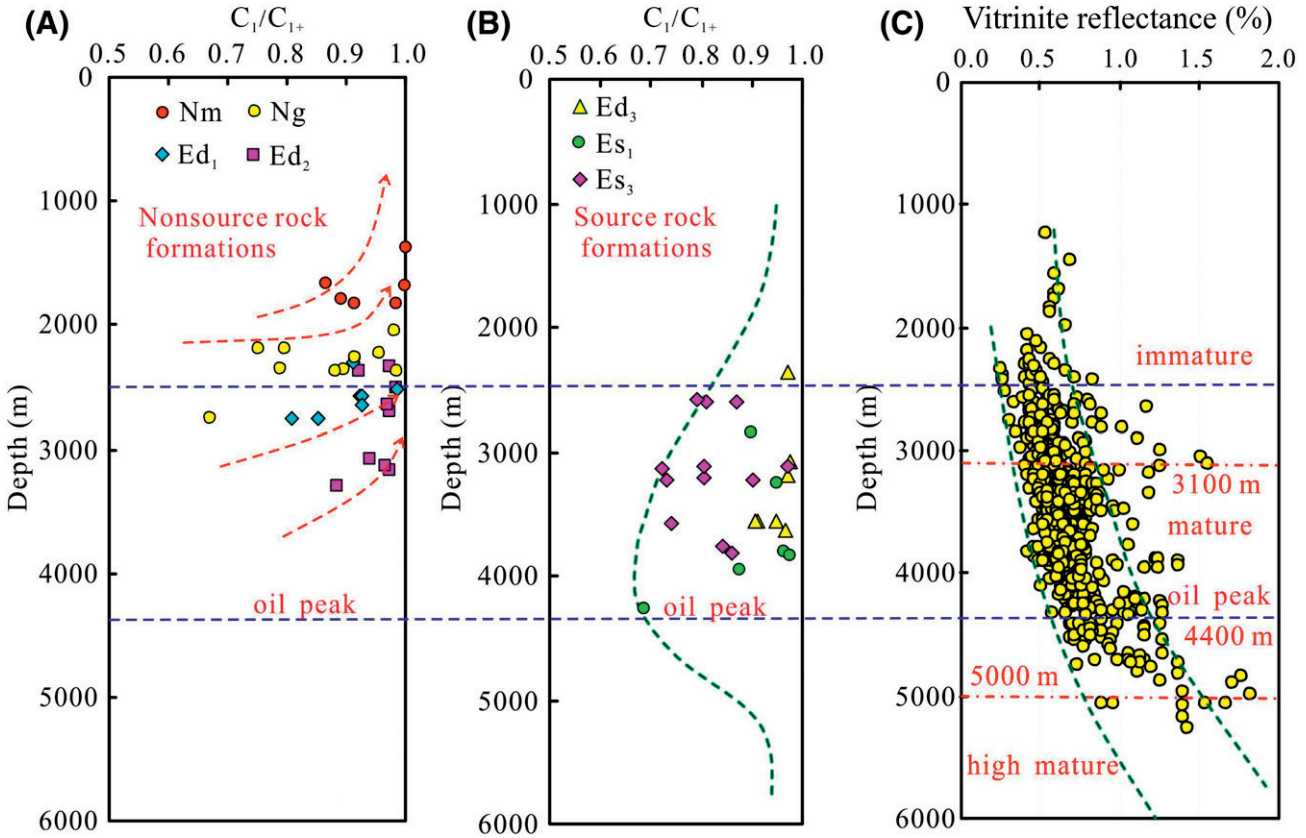

Figure 17. Scatter plots of the natural gas drying coefficient (C_1/C_{1+}) versus depth of the Neogene Minghuazhen Formation (Nm), Neogene Guantao Formation (Ng), first and second members of the Dongying Formation (Ed_1 and Ed_2) (A), and third member of the Dongying Formation (Ed_3), first member of the Shahejie Formation (Es_1), and third member of the Shahejie Formation (Es_3) (B) as well as vitrinite reflectance (%) versus depth (C) in the Nanpu sag.

sag, corresponding to the thicker part of the Es_1 source rock (Figure 19B).

The Ed_3 source rock has a moderate thickness, and the thickest part is distributed in the south of the Gaoshangpu SB. In addition, the type B oil is in or around the thick (Figure 19C). Based on the analysis mentioned above, the different types of oils are all associated with the thicker part of the corresponding source rocks.

In the Nanpu sag, most of the hydrocarbons have been discovered in the layers above the source rocks.

Table 3. Characteristics of the Gas-to-Oil Ratios for the Different Structural Belts in the Nanpu Sag

Formation	Liuzan, m^3/t	Gaoshangpu, m^3/t	Laoyemiao, m^3/t	Offshore, m^3/t
Nm	19–947; 261 (14)	6–992; 149 (56)	8–808; 230 (7)	59–1211; 423 (5)
Ng	13–603; 136.9 (12)	14–611; 130 (14)	19–4293; 724 (60)	47–2654; 623 (16)
Ed_1	–	40–4372; 713 (22)	261–395; 295 (3)	48–2372; 877 (21)
Ed_2	–	606–606; 606 (1)	225–1010; 652 (3)	–
Ed_3	–	40–3050; 489 (12)	40–2474; 845 (3)	–
Es_3	11–10,362; 563 (56)	33–5608; 569 (60)	–	–

Minimum to maximum; average (samples).

Abbreviations: – = not applicable; Ed_1 = first member of the Dongying Formation; Ed_2 = second member of the Dongying Formation; Ed_3 = third member of the Dongying Formation; Es_3 = third member of the Shahejie Formation; Ng = Neogene Guantao Formation; Nm = Neogene Minghuazhen Formation.

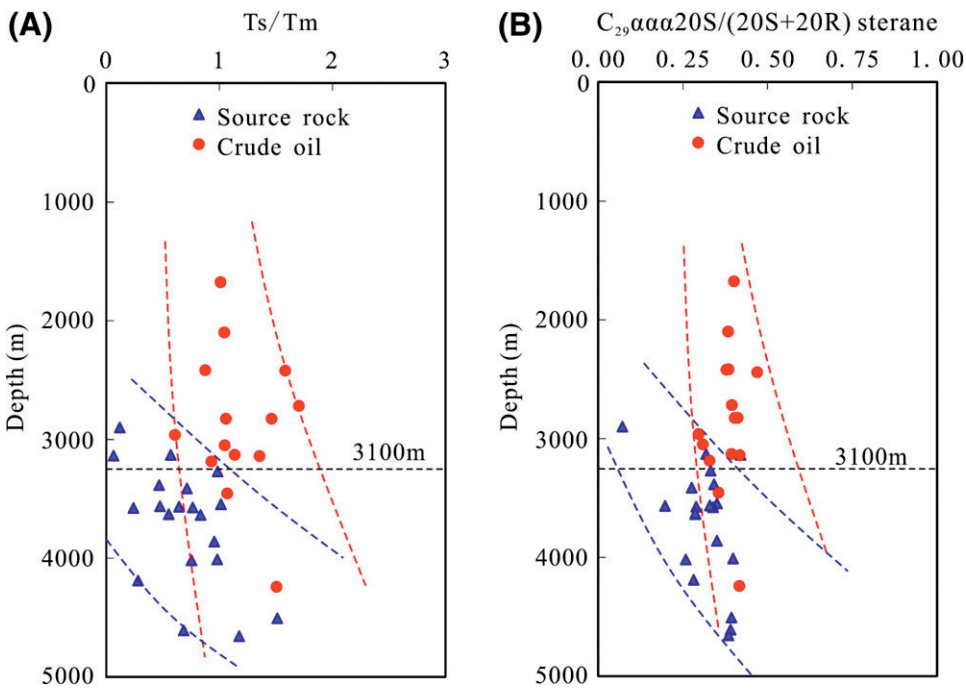

Figure 18. Scatter plots of C_{27} 18α (H),22,29,30-trisnorneohopane/C_{27} 17α (H),22,29,30-trisnorhopane (Ts/Tm) (A) and C_{29}ααα20S/(20S+20R) sterane (where S indicates left-handed stereo configuration and R indicates right-handed stereo configuration) (B) versus depth for the source rock and crude oils in the Nanpu sag.

This finding means that there is a clear vertical migration along faults. The hydrocarbons mainly occur in the areas where the faults and source rocks overlap. Therefore, the hydrocarbon distribution is jointly controlled by both the source rock thickness and the adjacent faults in the Nanpu sag.

The natural gas was discovered either above or under the oil generation threshold in the Nanpu sag, with a depth interval of 3000–3500 m (~9840–11,480 ft) (Figure 17C). Based on the analytical results of the high-pressure physical properties for the crude oil in the reservoirs, the solution gas- (in oil) to-oil ratio decreases as burial depth decreases. From 3100 to 5000 m (~10,168–16,400 ft), the gas-to-oil ratio decreases rapidly because the gas comes out of the crude oil (Figure 20A). The gas coming from the crude oil is the prominent mechanism for the gas layer forming in the Nm, Ng, and Ed_1 (Gao et al., 2012). In the Nanpu sag, when the burial depth reaches the top of the oil window, large amounts of gases are dissolved in the crude oil, forming more gas layers in the upper part of the oil window (Figure 20B). At a depth of 1300–3000 m (~4264–9840 ft), the gas-to-oil ratio has a smaller decrease. This indicates that above the depth of 3000 m (9840 ft), only a small quantity of the dissolved gas comes from the crude oil. This is an important reason why there are fewer gas layers above the oil window's top depth (Figure 20B). Therefore, it is the exsolution of the dissolved gas in the oil that is an important condition for the formation of gas layers in the Nm, Ng, and Ed_1 of the Nanpu sag (Gao et al., 2011). The discovered natural gas in the Nanpu sag mainly occurs as dissolved gas in oil and free gas. The free gas came from the exsolution of the dissolved gas.

Based on the relationship between the source rock evolution and the distribution depth of the oil and gas, it is speculated that there will still be considerable oil to be found in the depth range of the oil window and more gas or light oil within the depth range of the oil window, even in the deeper sections (Figure 20C).

CONCLUSIONS

1. The discovered oils are mainly distributed in the Nm, Ng, and Ed_1 in the whole Nanpu sag. But the Es_3 oil layer is chiefly distributed in the Liuzan

Table 4. Biomarker Characteristics of the Shale and Oil in the Nanpu Sag

Well	Depth, m	Formation	Shale/Oil	$C_{29}\alpha\alpha\alpha$20S/(20S+20R) Sterane	Ts/Tm
G190X1	4010.0	Es_3	Shale	0.40	0.98
B2X1	3574.8	Ed_3	Shale	0.29	0.76
B30	3634.8	Ed_2	Shale	0.29	0.84
LBN1	3544.0	Es_1	Shale	0.35	1.01
NP1	3386.0	Ed_3	Shale	0.34	0.47
Lao2X1	4506.6	Ed_3	Shale	0.39	1.51
JH1X1	3129.0	Ed_1	Shale	0.32	0.57
NP1	3859.0	Es_1	Shale	0.35	0.96
NP5-81	4606.0	Es_3	Shale	0.39	0.68
L31-4	3270.0	Es_3	Shale	0.33	0.98
NP1	4655.0	Es_2	Shale	0.39	1.17
NP511	3566.6	Ed_3	Shale	0.20	0.64
NP5X6	3414.4	Ed_3	Shale	0.28	0.71
B6X1	3138.3	Ed_2	Shale	0.42	0.06
L35-4	2900.9	Es_3	Shale	0.07	0.12
B2X1	3575.2	Ed_3	Shale	0.34	0.24
G25-1	4187.8	Es_1	Shale	0.28	0.28
Gc1	3630.0	Es_3	Shale	0.29	0.55
B30	3564.0	Ed_2	Shale	0.33	0.48
G62	4018.4	Es_3	Shale	0.26	0.75
G29X6	3141.0	Ed_3	Oil	0.42	1.35
G78	2963.6	Es_2	Oil	0.30	0.61
L202X2	2441.9	Es_3	Oil	0.47	5.32
JH1X1	3186.2	Ed_1	Oil	0.33	0.93
Lao2X1	4241.6	Ed_2	Oil	0.42	1.50
NP101	1677.9	Nm	Oil	0.40	1.01
NP11-B45-X503	2416.8	Ed_1	Oil	0.39	0.87
NP1-5	2717.3	Ed_1	Oil	0.39	1.70
NP203X1	2825.2	Ed_1	Oil	0.40	1.06
NP2-1	2099.6	Ng	Oil	0.38	1.04
NP2-53	3129.4	Ed_1	Oil	0.39	1.14
LP1	3049.6	Ed_1	Oil	0.31	1.05
NP4-1	2419.8	Ng	Oil	0.38	1.58
NP503	3453.0	Ed_3	Oil	0.36	1.07
NP5-11	2825.3	Ed_3	Oil	0.41	1.46

Shale: source rock samples; oil: crude oil samples.

Abbreviations: Ed_1 = first member of the Dongying Formation; Ed_2 = second member of the Dongying Formation; Ed_3 = third member of the Dongying Formation; Es_1 = first member of the Shahejie Formation; Es_2 = second member of the Shahejie Formation; Es_3 = third member of the Shahejie Formation; Ng = Neogene Guantao Formation; Nm = Neogene Minghuazhen Formation; Ts/Tm = C_{27} 18α (H),22,29,30-trisnorneohopane/C_{27} 17α (H),22,29,30-trisnorhopane.

and Gaoshangpu SBs. The natural gases are mainly distributed in the Ed_3. The oil and gas are distributed around the source kitchen in a ring-like shape. The natural gases are closer to the sag center, whereas the oils migrate to the margin of the subsag with a longer lateral migration distance.

2. The crude oil is mainly light and medium in density. Some heavy oils occurring in the shallow layers are a result of biodegradation and oxidation in the onshore Liuzan, Gaoshangpu, and Laoyemiao SBs. The crude oils can be divided into four types: A, B, C, and D. The type A and D oils are sourced

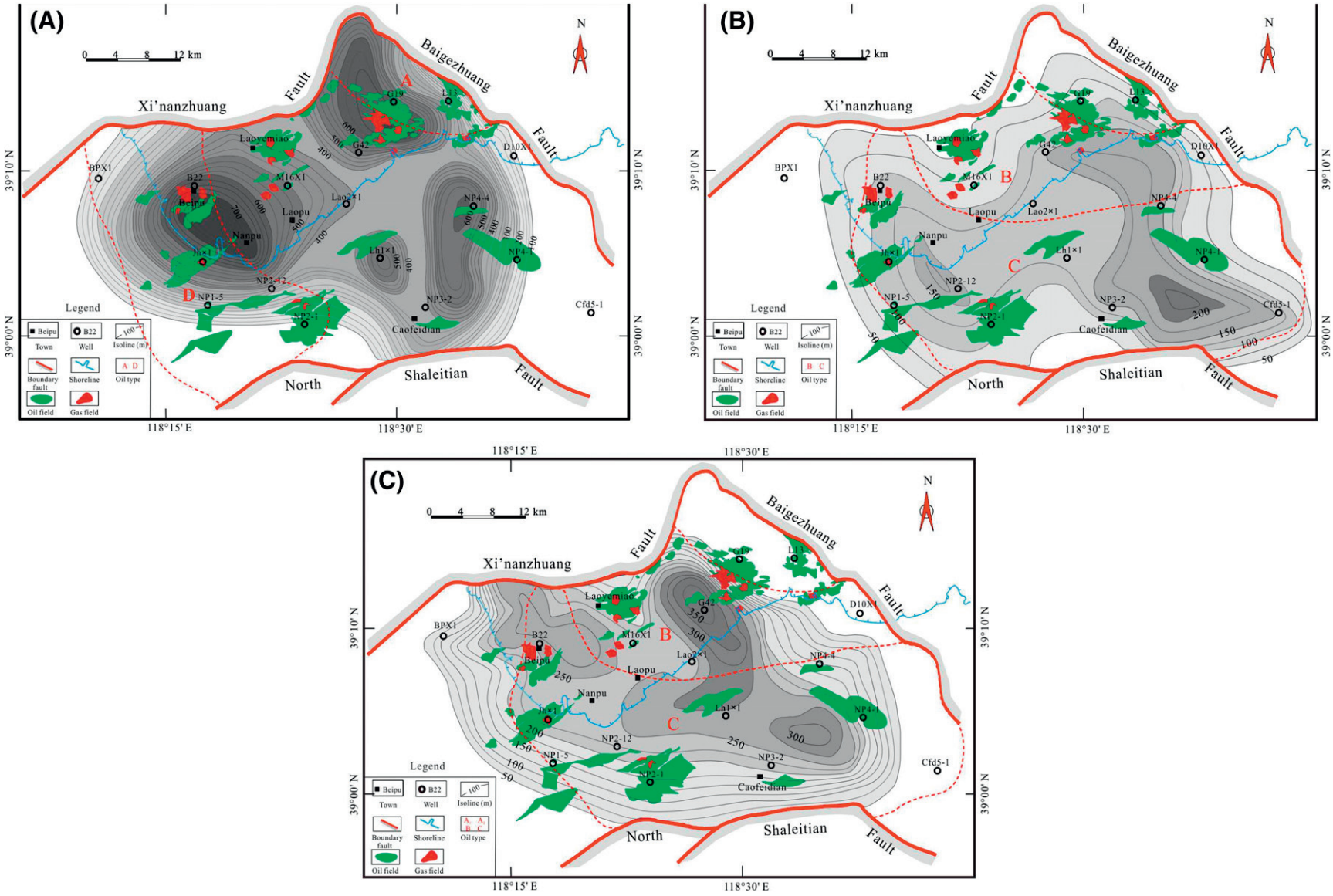

Figure 19. Superimposed map of the type A and D oils and the third member of the Shahejie Formation source rock (A); type B and C oils and first member of the Shahejie Formation source rock (B); type B and C oils and third member of the Dongying Formation source rock (C) in the Nanpu sag. Contour interval = 25 m.

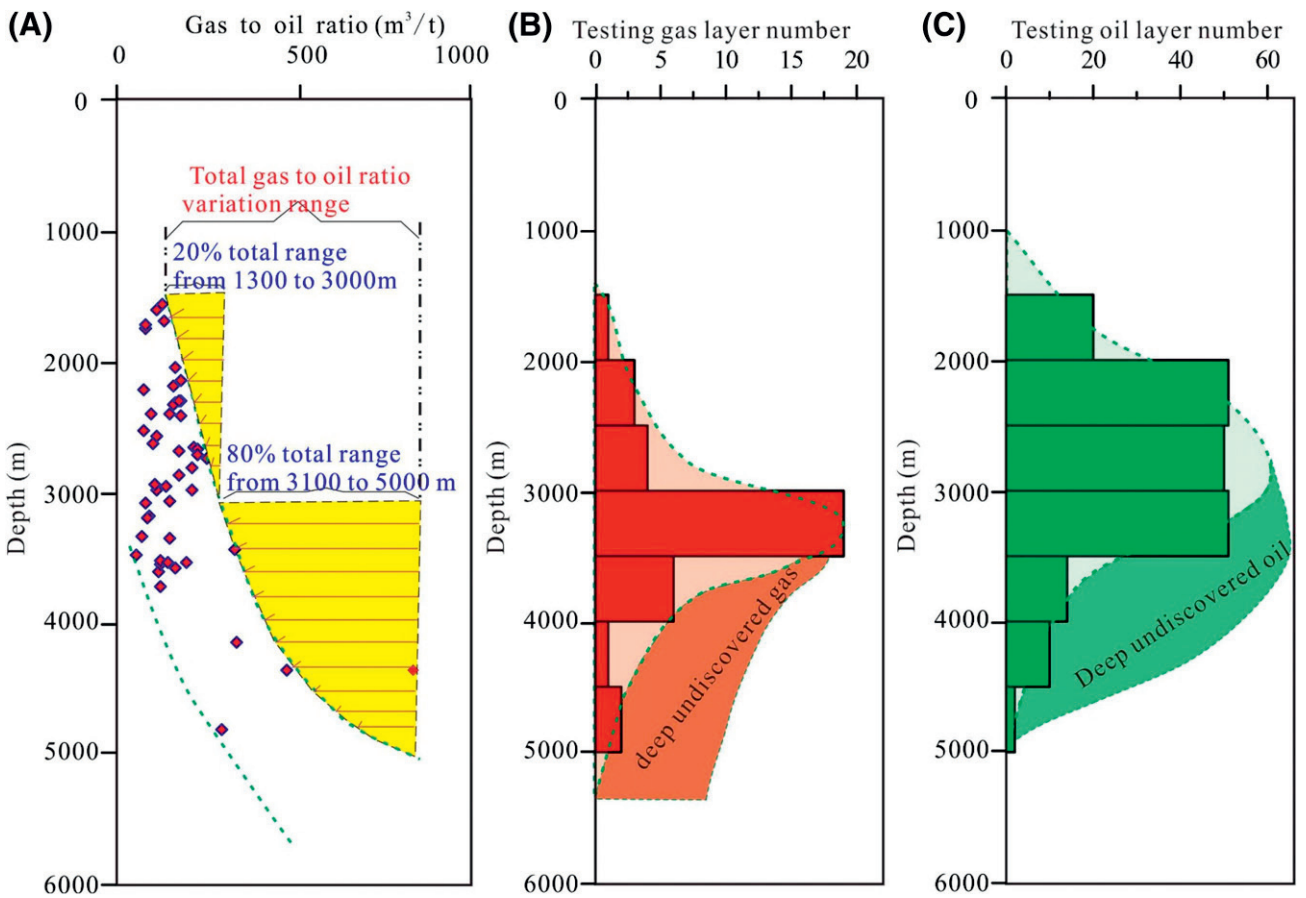

Figure 20. Plots of the gas-to-oil ratio (A), testing gas (B), and oil layers number (C) versus depth in the Nanpu sag.

from the Es_3 source rock, whereas the type B and C oils are mainly derived from the Ed_3 and Es_1 source rocks.

3. Based on the information provided by crude oil and source rock biomarkers, the oil-source correlation in Bohai Bay Basin was analyzed. The oil and gas show clear signs of vertical migration. The areas with thick source rock and abundant faults are favorable zones for oil and gas distribution, which reflects the general characteristics of oil and gas migration, accumulation, and preservation in rift basin. With the continuous discovery of large oil fields in rift basins globally, this study provides a reliable way to understand the potential of oil and gas exploration in a rift basin.

REFERENCES CITED

Adegoke, A. K., W. H. Abdullah, M. H. Hakimi, and B. M. Sarki Yandoka, 2014, Geochemical characteristics of Fika formation in the Chad (Bornu) Basin, northeastern Nigeria: Implications for depositional environment and tectonic setting: Applied Geochemistry, v. 43, p. 1–12, doi:10.1016/j.apgeochem.2014.01.008.

Ayala, L. F., T. Ertekin, and M. Adewumi, 2007, Numerical analysis of multi-mechanistic flow effects in naturally fractured gas-condensate systems: Journal of Petroleum Science Engineering, v. 58, no. 1–2, p. 13–29, doi:10.1016/j.petrol.2006.11.005.

Chen, X. F., S. M. Li, Y. X. Dong, X. Q. Pang, Z. J. Wang, M. S. Ren, and H. C. Zhang, 2016, Characteristics and genetic mechanisms of offshore natural gas in the Nanpu Sag, Bohai Bay Basin, eastern China: Organic Geochemistry, v. 94, p. 68–82, doi:10.1016/j.orggeochem.2016.01.011.

Clayton, C. J., 1991, Effect of maturity on carbon isotope ratios of oils and condensates: Organic Geochemistry, v. 17, no. 6, p. 887–899, doi:10.1016/0146-6380(91)90030-N.

Dong, Y. X., L. Xiao, H. M. Zhou, C. Z. Wang, and J. P. Zheng, 2010, The Tertiary evolution of the prolific Nanpu Sag of Bohai Bay Basin, China: Constraints from volcanic records and tectono–stratigraphic sequences: Geological Society of America Bulletin, v. 122, no. 3–4, p. 609–626, doi:10.1130/B30041.1.

Dong, Y. X., H. M. Zhou, and W. C. Xia, 2003, Relationship between Tertiary sequence stratigraphy and oil reservoir in Nanpu Sag: Oil & Gas Geology, v. 24, p. 39–42.

Gao, G., Z. L. Huang, B. J. Huang, J. Yuan, and C. X. Tong, 2012, The solution and exsolution characteristics of natural gas components in water at high temperature and pressure and their geological meaning: Petroleum Science, v. 9, no. 1, p. 25–30, doi:10.1007/s12182-012-0178-9.

Gao, G., Z. L. Huang, B. H. Liu, and H. C. Fan, 2011, Natural gas occurrence and distribution pattern of Western Sag of Liaohe exploration area: Zhongguo Shiyou Kantan, v. 1, p. 41–50, doi:10.3969/j.issn.1672-7703.2011.01.008.

Guo, Y. C., X. Q. Pang, Y. X. Dong, Z. X. Jiang, D. X. Chen, and F. J. Jiang, 2013, Hydrocarbon generation and migration in the Nanpu Sag, Bohai Bay Basin, eastern China: Insight from basin and petroleum system modeling: Journal of Asian Earth Sciences, v. 77, p. 140–150, doi:10.1016/j.jseaes.2013.08.033.

Head, I. M., D. M. Jones, and S. R. Later, 2003, Biological activity in the deep subsurface and the origin of heavy oil: Nature, v. 426, no. 6964, p. 344–352, doi:10.1038/nature02134.

Huang, W. Y., and W. G. Meinschein, 1979, Sterols as ecological indicators: Geochimica et Cosmochimica Acta, v. 43, no. 5, p. 739–745, doi:10.1016/0016-7037(79)90257-6.

Jiang, F. J., D. Chen, J. Chen, Q. W. Li, Y. Liu, X. H. Shao, T. Hu, and J. X. Dai, 2016a, Fractal analysis of shale pore structure of continental gas shale reservoir in the Ordos Basin, NW China: Energy & Fuels, v. 30, no. 6, p. 4676–4689, doi:10.1021/acs.energyfuels.6b00574.

Jiang, F. J., D. Chen, Z. F. Wang, Z. Y. Xu, J. Chen, L. Liu, Y. Y. Huyan, and Y. Liu, 2016b, Pore characteristic analysis of a lacustrine shale: A case study in the Ordos Basin, NW China: Marine and Petroleum Geology, v. 73, p. 554–571, doi:10.1016/j.marpetgeo.2016.03.026.

Jiang, F. J., X. Q. Pang, J. Bai, X. H. Zhou, J. P. Li, and Y. H. Guo, 2016c, Comprehensive assessment of source rocks in the Bohai Sea area, eastern China: AAPG Bulletin, v. 100, no. 6, p. 969–1002, doi:10.1306/02101613092.

Jiang, H., H. Wang, and Z. L. Lin, 2009, Periodic rifting activity and its controlling on sedimentary filling of Paleogene period in Nanpu Sag: Acta Sedimentologica Sinica, v. 27, no. 5, 976–982.

Killops, S. D., and M. A. Al-Juboori, 1990, Characterization of the unresolved complex mixture (UCM) in the gas chromatograms of biodegraded petroleum: Organic Geochemistry, v. 15, no. 2, p. 147–160, doi:10.1016/0146-6380(90)90079-F.

Köhler, J., and A. Clausing, 2000, Taxonomy and paleoecology of dinoflagellate cysts from upper Oligocene freshwater sediments of Lake Enspel, Westerwald area, Germany: Review of Palaeobotany and Palynology, v. 112, no. 1–3, p. 39–49, doi:10.1016/S0034-6667(00)00034-8.

Li, H. Y., Z. X. Jiang, and Y. X. Dong, 2010, Control of faults on hydrocarbon migration and accumulation in Nanpu Sag, Bohai Bay Basin: Geoscience, v. 24, p. 754–760.

Li, S. M., Z. X. Jiang, and Y. X. Dong, 2008, Genetic type and distribution of the oils in the Nanpu Sag, Bohai Bay Basin: Geoscience, v. 22, p. 818–822.

Liu, D. Z., J. Y. Zhou, and L. Ma, 2009, Study on the features of fault controlling pool in Nanpu Sag: Bohai Bay Basin: Offshore Oil, v. 29, p. 19–25.

Mei, L., Z. H. Zhang, and Y. Y. Fan, 2009, Geochemical characteristics of Es_4^3 source rocks and its oil source contribution in Nanpu Sag, Bohai Bay Basin: Natural Gas Geoscience, v. 20, p. 961–968.

Mei, L., Z. H. Zhang, and X. D. Wang, 2008, Geochemical characteristics of crude oil and oil source correlation in Nanpu Sag: Bohai Bay Basin: Journal of China University of Petroleum, v. 32, p. 40–47.

Pápay, J., 2003, Development of petroleum reservoirs: Theory and practice: Budapest, Hungary, Akademiai Kiado Publishers, 939 p.

Saberi, M. H., and A. R. Rabbani, 2015, Origin of natural gases in the Permo-Triassic reservoirs of the Coastal Fars and Iranian sector of the Persian Gulf: Journal of Natural Gas Science and Engineering, v. 26, p. 558–569, doi:10.1016/j.jngse.2015.06.045.

Shi, G. Z., H. Wang, and B. Xu, 2011, Activity of Baigezhuang fault of Nanpu Sag and its controlling on sedimentation: Acta Scientiarum Naturalium Universitatis Pekinensis, v. 47, p. 85–92.

Tong, H. M., B. Y. Zhao, Z. Cao, G. X. Liu, X. M. Dun, and D. Zhao, 2013, Structural analysis of faulting system origin in the Nanpu Sag, Bohai Bay Basin: Acta Geologica Sinica, v. 87, no. 11, p. 1647–1661.

Volkman, J. K., S. M. Barrett, S. I. Blackburn, M. P. Mansour, E. L. Sikes, and F. Gelin, 1998, Microalgal biomarkers: A review of recent research developments: Organic Geochemistry, v. 29, no. 5–7, p. 1163–1179, doi:10.1016/S0146-6380(98)00062-X.

Wan, T., Y. L. Jiang, and Y. X. Dong, 2012, Relationship between fault activity and hydrocarbon accumulation and enrichment in Nanpu Sag: Journal of China University of Petroleum, v. 36, p. 60–68.

Wang, Z. C., and H. J. Zheng, 2008, Oil-gas exploration potential for above-source plays in Nanpu Sag: Petroleum Exploration and Development, v. 35, no. 1, p. 11–16, doi:10.1016/S1876-3804(08)60003-8.

Wenger, L. M., C. L. Davis, and G. H. Isaksen, 2002, Multiple controls on petroleum biodegradation and impact on oil quality: SPE Reservoir Evaluation and Engineering, v. 5, no. 5, p. 375–383, doi:10.2118/80168-PA.

Xu, A. N., Y. X. Dong, C. N. Zou, Z. C. Wang, H. J. Zheng, X. D. Wang, and Y. Cui, 2008, Division and evaluation of oil-gas prolific zones for litho-stratigraphic reservoirs in the Nanpu Sag: Petroleum Exploration and Development, v. 35, no. 3, p. 272–280, doi:10.1016/S1876-3804(08)60072-5.

Zhang, R. X., J. P. Li, Z. G. Liu, S. L. Liu, and H. N. Lu, 2010, The study of sequence stratigraphy characteristics and the bottom boundary of Guantao Formation in the middle area of Bohai Bay Basin: Offshore Oil, v. 30, p. 19–25.

Zhao, Y. D., L. F. Liu, and Z. H. Zhang, 2008, Source analysis of oils from the Ordovician in the shoal zone Nanpu Sag, BohaiBay Basin: Geoscience, v. 22, p. 264–273.

Zheng, H. J., Y. X. Dong, and X. D. Wang, 2007a, The generation and characteristics of source rocks in Nanpu oil-rich depression, Bohai Bay Basin: Natural Gas Geoscience, v. 18, p. 78–83.

Zheng, H. J., Y. X. Dong, and G. Y. Zhu, 2007b, High quality source rocks in Nanpu Sag: Petroleum Exploration and Development, v. 34, p. 385–392.